ARTICLE NO. 79-0129R

Dryden Lectureship in Research

Computational Aerodynamics Development and Outlook

Dean R. Chapman
Ames Research Center, NASA, Moffett Field, Calif.

Introduction

IT is an honor and challenge to present the Dryden Lecture in Research for 1979. Since my topic concerns a new trend in fluid mechanics, it should not be surprising that some aspects of this paper involve basic mechanics of turbulence, a field enriched by numerous contributions of Dr. Hugh L. Dryden. Having worked in related fields of fluid mechanics during past years, and long respected both his professional contributions and personal integrity, it is a special pleasure to present this Dryden lecture.

The field of computational fluid dynamics during recent years has developed sufficiently to initiate some changes in traditional methods of aerodynamic design. Both computer power and numerical algorithm efficiency are simultaneously improving with time, while the energy resource for driving large wind tunnels is becoming progressively more valuable. Partly for these reasons it has been advocated that the impact of computational aerodynamics on future methods of aircraft design will be profound.[1,2] Qualitatively, the changes taking place are not foreign to past experience in other fields of engineering. For example, trajectory mechanics and neutron transport mechanics already have been largely revolutionized by the computer. Computations rather than experiments now provide the principal source of detailed information in these fields. The amount of reactor experimentation required has been much reduced over former years; experiments now are performed mainly on clear, physically describable arrays of elements aimed at further confirmation of computational techniques; and better designs are achieved than with former experimental methods alone. Similar changes in the relative roles of experimental and computational aerodynamics are anticipated in the future.

There are three compelling motivations for vigorously developing computational aerodynamics. One is to provide important new technological capabilities that cannot be provided by experimental facilities. Because of their fundamental limitations, wind tunnels have rarely been able to simulate, for example, Reynolds numbers of aircraft flight, flowfield temperatures around atmosphere entry vehicles, aerodynamics of probes entering planetary atmospheres, aeroelastic distortions present in flight, or the propulsive-external flow interaction in flight. In addition, transonic wind tunnels are notoriously limited by wall and support interference; and stream nonuniformities of wind tunnels severely affect laminar-turbulent transition. Moreover, the dynamic-aerodynamic interaction between vehicle motion in flight and transition-dependent separated flow also is inaccessible to wind-tunnel simulation.[3] In still different ways ground facilities for turbomachinery experiments are limited in their ability, for example, to simulate flight inlet-flow nonuniformities feeding into a compressor stage, or to determine detailed flowfields between rotating blades. Numerical flow simulations, on the other hand, have none of these fundamental limitations, but have their own: computer speed and memory. These latter limitations are fewer, but previously have been much more restrictive overall because the full Navier-Stokes equations are of such great complexity that only highly truncated and approximate forms could be handled in the past. In recent years the Navier-Stokes equations have begun to yield under computational attack with the largest current computers. Since the fundamental limitations of computational speed and memory are rapidly decreasing with time, whereas the fundamental limitations of experimental facilities are not, numerical simulations offer the potential of mending many ills of wind-tunnel and turbomachinery experiments, and of providing thereby important new technical capabilities for the aerospace industry.

A second compelling motivation concerns energy conservation. The large developmental wind tunnels require large amounts of energy, whereas computers require comparatively

Dr. Dean R. Chapman is Director of Astronautics at the Ames Research Center. In this post, Dr. Chapman administers organizations conducting space flight projects. Dr. Chapman joined Ames as an aeronautical engineer in 1944. He received his B.S. and M.S. degrees from California Institute of Technology in 1944 and his Ph.D. from Cal Tech in 1948 under a National Research Council Fellowship. He has made fundamental contributions in aerodynamic flow separation at supersonic speeds, the effects of trailing edge bluntness on drag and lift, atmosphere entry physics, and the origin of tektites. In 1952, Dr. Chapman received the Lawrence Sperry Award of the Institute of Aeronautical Sciences for contributions to aeronautics. In 1959 he received a Rockefeller Public Service Award to conduct research for a year at the University of Manchester, England and at Jodrell Bank. In 1963 he was awarded the NASA medal for Exceptional Scientific Achievement for his work on tektites, atmosphere entry physics, and space mechanics. In 1971 he received the H. Julian Allen Award of the Ames Research Center for his tektite work. He was elected in 1975 to the U.S. National Academy of Engineering. He was appointed as 1978/79 Hunsaker Professor, an honorary professorship, at the Massachusetts Institute of Technology and presented the Dryden Research Lecture of the American Institute of Aeronautics and Astronautics. Dr. Chapman is author of numerous technical papers and an AIAA Fellow.

Presented as Paper 79-0129 at the AIAA 17th Aerospace Sciences Meeting, Jan. 15-17, 1979; submitted March 17, 1979; revision received Sept. 5, 1979.

Index categories: Computational Methods; Aerodynamics; Computer Technology.

negligible amounts. In coming years, energy considerations are anticipated to impose significant restrictions on testing time in large wind tunnels. Thus the development of computational aerodynamics and advanced computers is expected to lessen considerably the potential impact of such restrictions.

The third major motivation for developing computational aerodynamics relates to economics. Since computer speed has increased with time at a much greater rate than computer cost, the net cost to conduct a given numerical simulation with a fixed algorithm has decreased rapidly with time (Fig. 1). In addition, the rate of improvement in the computational efficiency of numerical algorithms for a given computer has been equally remarkable. This is illustrated in Fig. 2 comparing the trend in relative computation cost due to computer improvements alone with the corresponding trend due to algorithm improvements alone. The two trends have compounded to bring about an altogether extraordinary cost-reduction trend in computational aerodynamics. The cost of experiments, in contrast, has been increasing with time.

An example may suffice to illustrate the dramatic trend in computation efficiency. A numerical simulation of the flow over an airfoil using the Reynolds averaged Navier-Stokes equations can be conducted on today's supercomputers in less than a half hour for less than $1000 cost in computer time. If just one such simulation had been attempted 20 years ago on computers of that time (e.g., the IBM 704 class) and with algorithms then known, the cost in computer time would have amounted to roughly $10 million, and the results for that single flow would not be available until 10 years from now, since the computation would have taken about 30 years to complete.

The objectives of this paper are to review some of the major developments in computational aerodynamics of the past decade, to assess critically what demands will be placed on future computer power by advanced flow simulation, to survey some trends in microelectronics upon which future computer power depends, and finally, to form therefrom some estimates of what new computational capability may be realized in the coming decade or so.

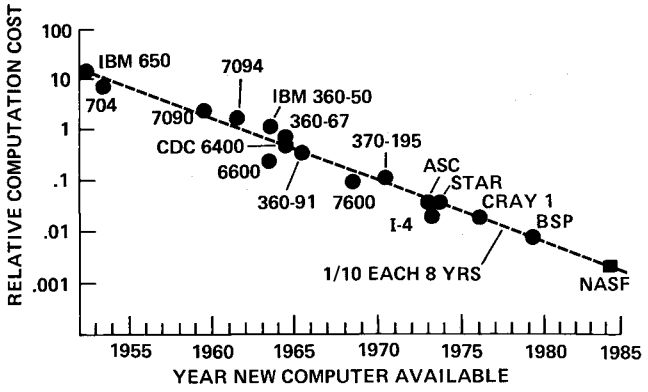

Fig. 1 Trend of relative computation cost for numerical flow simulation on large computers; given flow and algorithm.

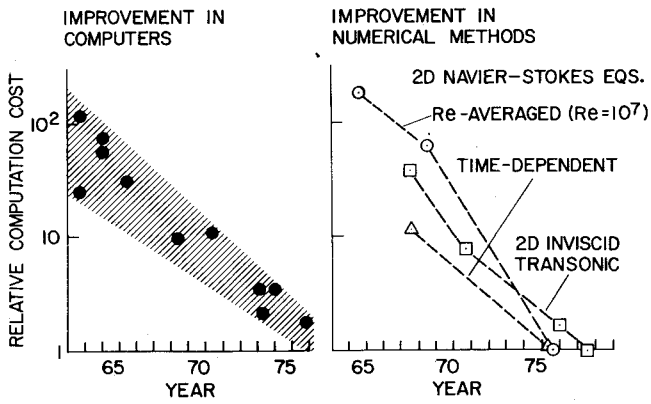

Fig. 2 Cost effectiveness improvements in computer hardware and in numerical methods.

Development of Computational Aerodynamics

Historical progress in computational aerodynamics can be characterized by a series of steps, each representing a successively refined approximation to the full Navier-Stokes equations. Four major stages of approximation stand out in order of their evolution and complexity: (I) linearized inviscid, (II) nonlinear inviscid, (III) Reynolds averaged Navier-Stokes, and (IV) full Navier-Stokes. Progressive advances in computer power and in numerical methods have made possible the development of a variety of computational codes ranging from Stage I codes for complex aircraft configurations to Stage IV codes for very simple geometry. With a given stage of approximation these advances have also enabled flow simulations to be made for successively more complex geometric configurations. Moreover, each new stage of approximation allows a new class of physical phenomena to be simulated: for example, subsonic lift distribution in Stage I, transonic wave drag in Stage II, airfoil buffeting in Stage III, boundary-layer transition and aerodynamic noise in Stage IV. The development of a code using a new stage of approximation does not diminish the practical utility of older, more approximate codes. Since refined approximations to the Navier-Stokes equations require increased computing time, codes based on the simplest applicable approximation remain useful.

Inviscid aerodynamic computations for two-dimensional airfoils were initiated in the first decade of this century. Numerical flowfield simulations for complex three-dimensional aircraft, however, were not developed until the 1960's when computers first made this possible using the linearized inviscid approximation of Stage I. The practical development of the nonlinear approximation of Stage II began in 1970, while intensive research development of Stage III has proceeded since 1974. Stage IV for turbulent flow is in an early phase of research. A summary of some major developmental milestones for the past and anticipated future is presented in Table 1. In general, each new stage becomes practical when the requisite computer power for that stage becomes available. Each generation of computer provides both engineering design computations with a given stage of approximation and research computations with an advanced stage of approximation. In the paragraphs which follow, some representative examples are illustrated for each of the four stages of development.

Stage I—Linearized Inviscid

Numerical computation methods using this stage of approximation are termed "panel methods" inasmuch as complex aircraft geometries are modeled by a large number of contiguous surface panels. Whereas the full Navier-Stokes equations representing conservation of mass, momentum, and energy contain altogether 60 partial-derivative terms when written out in three Cartesian coordinates, the linearized inviscid approximation truncates this to the well-known potential wave equation containing only 3 terms. It is remarkable that such a seemingly crude approximation turns out to be so practically useful. For subsonic subcritical flow over bodies without flow separation, panel methods provide realistic determinations of pressure distribution, of lift and side forces, of pitch, yaw and roll moments, and of induced vortex drag. For supersonic flow over slender bodies, wave drag is also determined. Having been under development for over a decade now, this stage of approximation is relatively mature (cf., for example, Refs. 4-7). An excellent survey of

Table 1 Development of computational aerodynamics

Stage	Computed results	Readiness time period: 2-D Airfoil B. of R.	Simple 3-D B. of R. at α wing	Practical 3-D wing-body	Computer class for practical 3-D calculations
I Linearized Inviscid	Pressure distribution Vortex drag Supersonic wave drag	1930	1940's	1968	IBM 360 CDC 6600
II Nonlinear Inviscid	Above plus: Transonic flow Hypersonic flow	1971	1973	1976	Current supercomputers
III Navier-Stokes Re-averaged Model all scales of turbulence	Above plus: Separated flow Total drag Performance Buffeting, buzz	1975	1978	Early 1980's	40 × current supercomputers (NASF)
IV Large eddy simulation Model subgrid- scale turbulence	Above plus: Aerodynamic noise Transition Surface pressure fluctuations	Early 1980's	Mid 1980's	1990's	At least 100 × NASF

some practical use of panel methods has recently been given by da Costa.[8]

An example of the linearized inviscid panel method is illustrated in Fig. 3 for the shuttle orbiter mounted on top of the B747 carrier aircraft.[8] Roughly 1000 panels were used for this configuration. Accurate determinations were made of the lift characteristics for the combined configuration and for each vehicle during separation of the orbiter from the carrier. Configuration orientations selected from the computational design phase were tested in the wind tunnel for verification.

An example from Kraus[7] is shown in Fig. 4. Here panel methods were used to compute forces and moments on the external stores mounted beneath the F4 wing. In this case, the agreement with experiment is less precise perhaps due to more intricate geometry and greater viscous effects. The degree of geometric detail resolvable by panel methods is limited by computer speed, since the computation time varies with the number of panels n as somewhere between n^2 and n^3. Improved computer power in the future, of course, will make practical increased geometric resolution.

State II—Nonlinear Inviscid

In its full complexity, this stage of approximation neglects only viscous terms and contains 27 of the 60 partial-derivative terms in the complete Navier-Stokes equations. Both transonic and hypersonic codes have been developed within this general framework of approximation. Transonic simulations will be discussed first.

Prior to the development of electronic computers, very few computations were made of practical transonic flowfields. Hand relaxation techniques were used by Emmons[9] to compute the supercritical transonic flow over a nonlifting airfoil and by Vincenti and Wagoner[10] to compute the transonic flow over a lifting double-wedge airfoil with detached bow wave. To this writer's knowledge, the first transonic solution for a practical lifting airfoil with embedded shock was published in 1970 by Magnus and Yoshihara[11] who used an explicit time-dependent method.

Vigorous activity erupted a year later with four separate publications on airfoils[12-15] and one on bodies of revolution including computations of wind-tunnel wall and support interference effects.[16] All employed relaxation procedures. Some used the small perturbation approximation and were followed by numerical solutions for wings,[17] wing-body combinations,[18] and artillery projectiles at angle of attack.[19] Others used the full potential equation and, generally with a 2- to 3-year lag, developed codes for bodies of revolution at zero angle of attack,[20] wings,[21] axisymmetric inlets at angle of attack,[22] and, finally, for wing-cylinder combinations.[23,24] An example of Stage II approximation from the first tran-

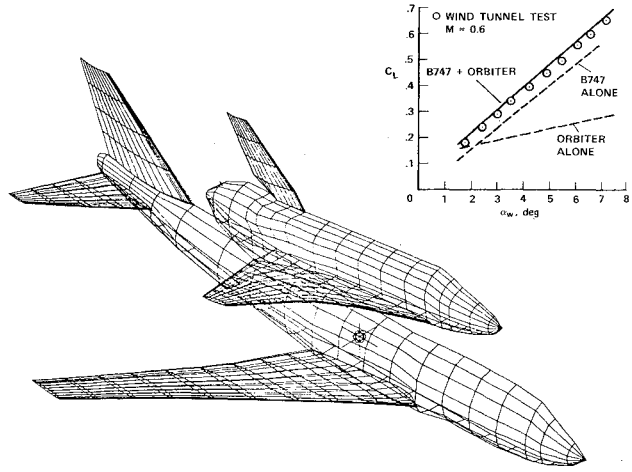

Fig. 3 Computer paneling of Space Shuttle Orbiter mounted on B747; linearized inviscid flow computation from da Costa (1978).

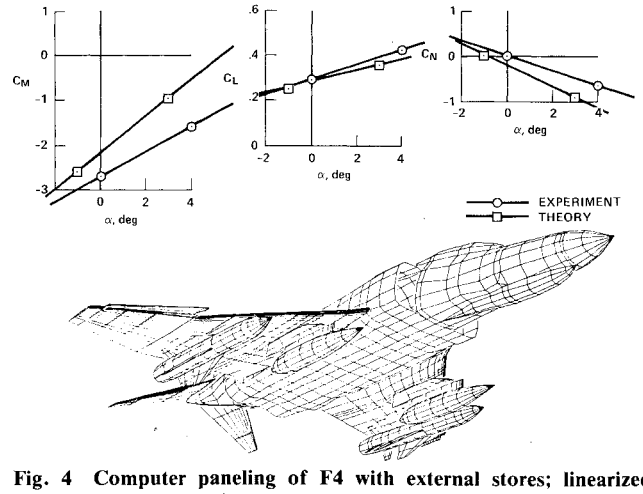

Fig. 4 Computer paneling of F4 with external stores; linearized inviscid flow computation, $M = 0.7$, from Kraus (1978).

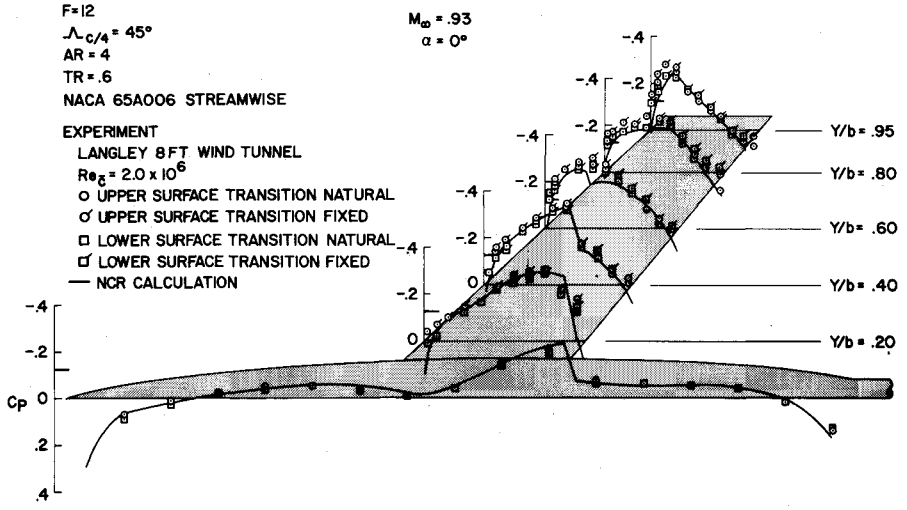

Fig. 5 Comparison of computed and measured pressure distributions on a swept-wing fuselage with sting support; nonlinear inviscid flow computation from Bailey and Ballhaus (1975).

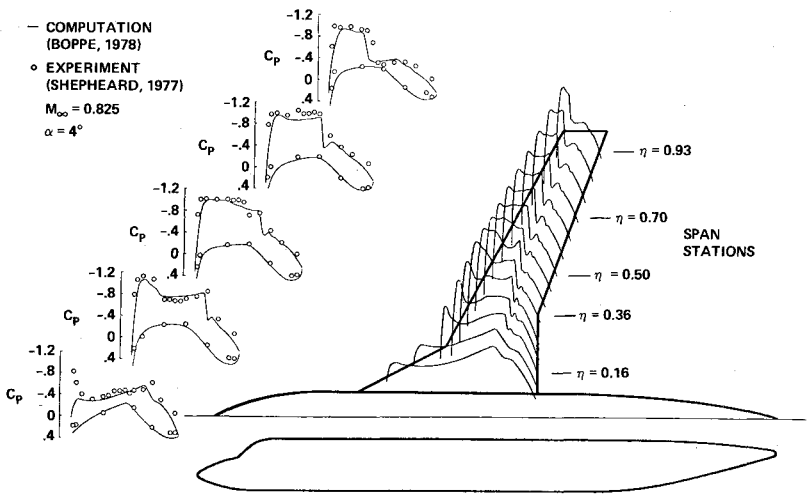

Fig. 6 Comparison of computed and measured pressure distributions for a supercritical wing with fuselage; nonlinear inviscid flow computation from Boppe (1978).

sonic simulation of a wing-body combination (Ref. 18) is presented in Fig. 5. This configuration, which includes the model support sting, is sufficiently slender that agreement between computation and experiment is uniformly good for both location and strength of the shock-wave system. Recently, implicit approximate factorization algorithms have been developed that converge more rapidly than relaxation schemes.[25,26] It is notable that in less than a decade following the initial computations of Magnus and Yoshihara, the efficiency of numerical methods for transonic flow has been improved by a factor of about 30 (Fig. 2). Currently, the best methods require the order of 10^4 floating-point operations per grid point, an amount that still leaves some room for further improvement.

Nonlinear inviscid computations for transonic flow, like linearized inviscid panel methods for subsonic flow, are now extensively used in the aircraft industry. A number of successful design applications has been made for transport aircraft, military fighters, business jets, missiles, and projectiles. In designing the HIMAT aircraft,[27] for example, the use of the Bailey-Ballhaus code enabled drag reduction of about 20% at maneuvering lift to be achieved relative to designs based on previous conventional methods. In a redesign of the wing of the North American Sabre 60 business aircraft,[28] the same code was used to achieve from 27 to 61% increase in range, 4 to 10% improvement in fuel consumption, and other significant improvements in take-off distance, cruise speed, and landing speed. Recently, Boppe[29] has illustrated how the use of nested grid systems makes it practical to construct transonic codes for arbitrary wing-fuselage configurations with winglets, pods, canards, and tails. An example from Boppe, comparing computations with experimental data for a fuselage with supercritical wing is shown in Fig. 6. The agreement is good for the small angle of attack investigated.

Some promising results have been obtained by combining numerical optimization techniques with nonlinear inviscid codes (e.g., Ref. 30 and references cited therein). Such techniques have the essential advantage over inverse methods of being able to consider automatically multiple-condition design problems wherein one aerodynamic characteristic is optimized while simultaneously imposing various other constraints—such as on off-design performance, and/or on volume, and/or on some structural parameter. In one example, a wing with variable leading- and trailing-edge camber, as optimized computationally,[31] provided somewhat higher L/D than corresponding configurations determined from conventional parameteric wind-tunnel tests. Such computational optimizations, of course, are significant only if transonic wave drag is a major part of total drag and if the flow does not involve strong viscous-inviscid flow interaction. Numerical optimization with future viscous-flow codes should open many new avenues for aerodynamic improvements.

The second type of nonlinear inviscid code developed is for hypersonic or purely supersonic flow. For such codes the Lax-Wendroff "shock-capturing" technique has been widely used.[32] One successful application[33] was to the "shock-on-shock" problem of determining the transient loads encountered when a supersonic/hypersonic missile flies through

a blast wave. Previous approximate methods of estimation gave widely disparate results. Experiments using a rocket-propelled test sled in combination with large shock tubes verified the computations. Significantly, the computations were completed prior to the experiments, cost much less, and provided more information.

Nonlinear inviscid codes for simulating hypersonic flow have been developed for the Shuttle Orbiter. Near peak entry heating this vehicle is enveloped by dissociated air that is chemically reacting and not in equilibrium. Laboratory experiments cannot be conducted at the scale of the orbiter and hence cannot accurately simulate nonequilibrium reaction-rate effects within the flowfield. The computer simulations for full-scale entry flight conditions[34] represent an example of using computational aerodynamics to simulate flows impossible to simulate in ground-based experimental facilities. In addition to this application, the supersonic/hypersonic codes of Stage II have been applied to maneuvering re-entry vehicles, supersonic aircraft, nozzle flows, inlets, and solar winds about planets.

There is no doubt that in the past few years the development of nonlinear inviscid codes for three-dimensional flows has provided a new technological capability for the aerodynamic design process. Moreover, it has shortened the design time and reduced costs considerably in some cases. In the HIMAT case, for example, Rockwell International Co. estimated that conventional transonic wind-tunnel tests of 10 wing designs they investigated computationally would have cost 26 times as much as the computations.

Stage III—Reynolds Averaged Navier-Stokes

Unlike the inviscid approximations, this approximation does not neglect any terms in the Navier-Stokes equations. The basic equations are averaged over a time interval which is long compared to turbulent eddy fluctuations yet small compared to macroscopic flow changes. Such a process introduces various new terms representing the time-average transport of turbulent momentum and energy. Since such terms must be modeled, the principal inaccuracy of Stage III is that of modeling turbulence. The primary merits of the approximation are that it provides in many cases realistic simulations of separated flows, of unsteady flows such as buffeting, and of total drag rather than only components of drag (e.g., induced drag in Stage I, wave drag in Stage II). Combined with computer optimization methods, these simulations should make it possible to develop aerodynamically optimum designs for realistic conditions of viscous compressible flow.

Numerical calculations for laminar flow using the complete Navier-Stokes equations can be viewed as a special subcase of Stage III simulations having zero turbulence. A number of laminar flow computations has been summarized in Ref. 35. One of the pioneering computations that led to important subsequent developments was the investigation by MacCormack[36] for shock-wave interaction with a laminar boundary layer. Other notable examples are the computation of laminar flow over a compression corner,[37] hypersonic flow over the front of blunt bodies,[38] incompressible flow over bluff bodies and airfoils,[39,40] and supersonic two-dimensional flow over a blunt body with an impinging shock wave.[41] The first three-dimensional aerodynamic simulation with the laminar Navier-Stokes equations apparently was of the flow over an inclined body of revolution.[42] Recently, similar numerical computations have been made of the laminar flow over three-dimensional compression corners.[43,44] Unsteady laminar flows have been limited to two dimensions, an impressive example of which is Mehta's[45] simulation of the dynamic stall of an airfoil oscillating at low Reynolds number. As expected, all of these computations agree well with experiments. A visual illustration from Mehta is shown in Fig. 7.

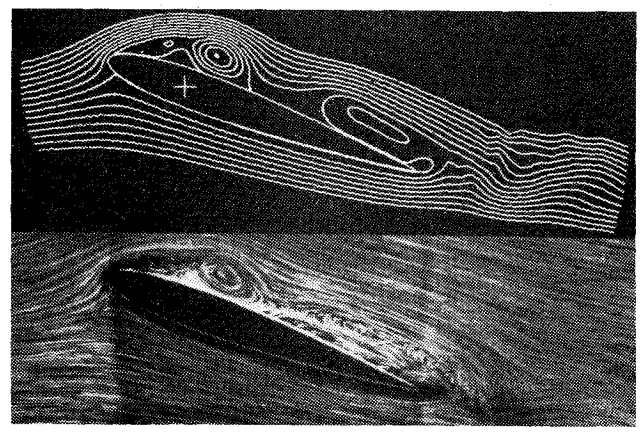

Fig. 7 Comparison of computed and observed unsteady flow over an oscillating airfoil at low *Re*; laminar viscous computation from Mehta (1977). $R = 5000$, $k = 0.5$, $\alpha = 20$ deg, second cycle.

The technology of simulating turbulent flows with the Reynolds averaged Navier-Stokes equations is relatively young, and most emphasis to date has been on two-dimensional flows. The first codes were developed for shock-wave interaction with a turbulent boundary layer (Refs. 46 and 47) and for high Reynolds number transonic flow over airfoils (Ref. 48). Numerical computations also have been made for supersonic flow over compression corners[49-51] and axially symmetric afterbodies.[52] Most of these employed relatively simple mixing length models for turbulence.

The possibility of using the Reynolds averaged Navier-Stokes equations to numerically simulate unsteady buffeting in transonic flow was first demonstrated by Levy.[53] He found that for a thick circular-arc airfoil the Reynolds averaged simulations automatically computed an unsteady flowfield at certain Mach numbers and steady flow at others. For Mach numbers below a critical value, the computed flow involved trailing-edge separation and was steady; for Mach numbers well above, it also was relatively steady but involved shock-induced separation; whereas for an intermediate Mach number range the flow oscillated violently between trailing-edge and shocked-induced separation. A comparison with experiment showed remarkable agreement for the frequency, the intensity, the Mach number of onset, and the time-dependent pressure variations at fixed positions along the airfoil chord.

Some recent numerical computations by H. Lomax, G. Deiwert, J. Steger, and H. Bailey of the drag polar and lift curve for a supercritical airfoil in transonic flow at high Reynolds number are presented in Fig. 8. These results (discussed by Peterson[54] and Deiwert and Bailey[55]) illustrate the computation of unsteady buffeting forces near and beyond maximum lift. In the corresponding wind-tunnel experiments,[56,57] two different amounts of wall porosity were employed in view of the uncertain effects of wind-tunnel wall interference. The computations for free-flight conditions differ less from the wind-tunnel results for the smaller wall porosity than the two experimental results differ from each other. This is believed to be an example of computer flow simulation probably providing a more accurate representation of free-flight aerodynamics than conventional wind-tunnel experiments. The buffet boundary computed at $C_L \simeq 0.85$ for $M_\infty = 0.75$ agrees closely with the experimental buffet boundary.[58]

Very recently Steger and Bailey[59] have used the Stage III Reynolds averaged Navier-Stokes equations to simulate aileron buzz. In 1947 it was discovered during wind-tunnel tests of a semispan wing of the P80 aircraft that severe control surface vibrations encountered earlier in flight tests represented a new type of flutter involving only one degree of mechanical freedom (Ref. 60). Steger and Bailey's simulation

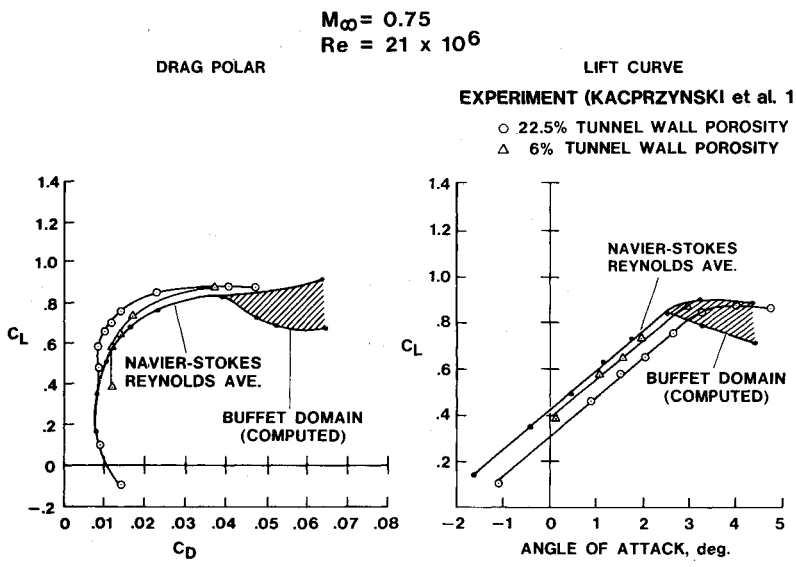

Fig. 8 Computed and measured transonic drag polar and lift curve for a supercritical airfoil; Reynolds averaged Navier-Stokes computation for turbulent flow from Deiwert and Bailey (1978).

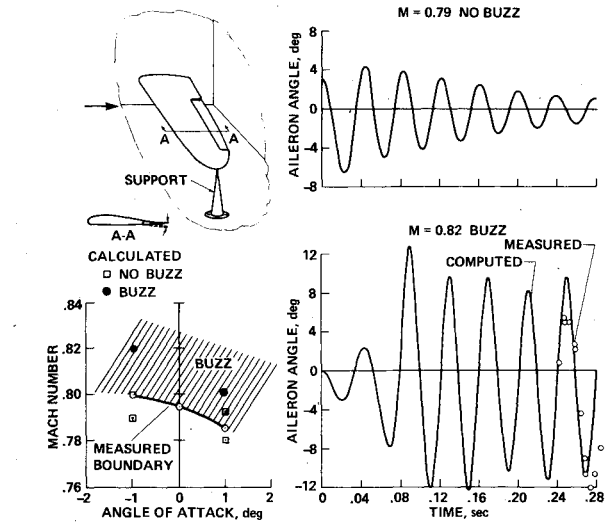

Fig. 9 Computed and measured characteristics of transonic aileron buzz; Reynolds averaged Navier-Stokes computation for turbulent flow from Steger and Bailey (1979).

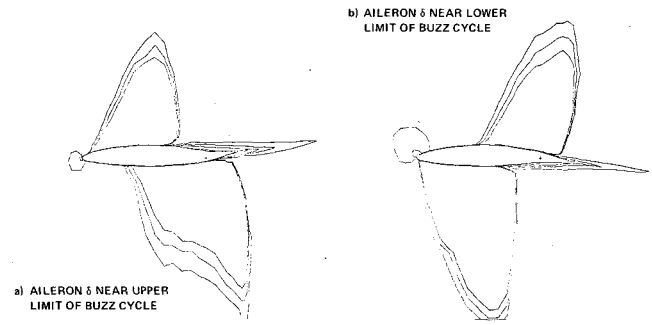

Fig. 10 Mach number contours of flowfields for transonic aileron buzz: $M_\infty = 0.82$, $\alpha = -1$ deg; Reynolds averaged Navier-Stokes computation for turbulent flow from Steger and Bailey (1979).

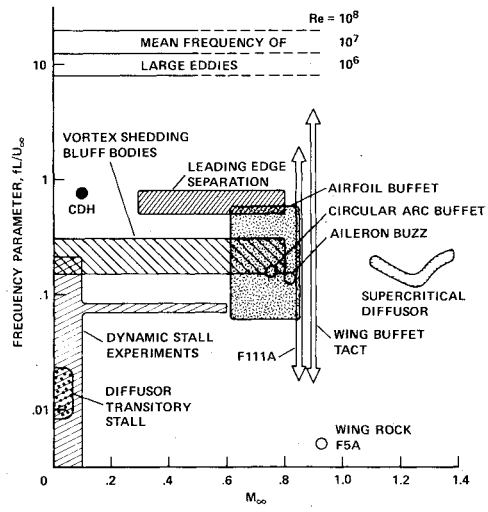

Fig. 11 Comparison of frequency range of unsteady flows with mean frequency of large-scale turbulent eddies.

of this classical experiment (Figs. 9 and 10) has revealed very good agreement for the Mach number of buzz onset and for both the frequency and amplitude of unsteadiness. It is important to note that in these computations, as in Levy's computations of airfoil buffeting, the computer codes without adjustment automatically produced unsteady flow when the experimental flow was unsteady and steady flow when the experimental flow was steady.

The investigations of unsteady flow have opened a broad new field for numerical simulation of aerodynamic phenomena previously intractable to detailed computation. While results to date have been encouraging, they also have raised at least two fundamental questions. One concerns how high the frequency of unsteadiness f can be relative to the mean frequency f_{te} of turbulent eddies for realistic simulations with the Reynolds averaged equations. The basic Reynolds concept involves averaging over a time interval long compared to the characteristic time f_{te}^{-1} of the principal turbulent eddies, yet short compared to the characteristic time f^{-1} of the unsteady mean flow. Thus f should be much smaller than f_{te}. In order to obtain a perspective on the question, some relevant data have been assembled in Fig. 11. Here the lines representing the mean frequency of turbulent eddies are based on flat-plate experiments (Refs. 61, 62, and references cited therein) and correspond to $U_\infty/\delta f_{te} \approx 5$. Also shown are the domains of some representative types of unsteady flow: airfoil buffet,[63,64] wing buffet,[65] leading edge separation,[66] vortex shedding behind bluff bodies,[67] supercritical diffusor stall,[68] low-speed diffusor transitory stall,[69] dynamic stall experiments,[70] and transonic wing rock.[71] It is clear that the frequencies of many unsteady flows of practical interest are a factor of 10 to 100 below the mean frequency f_{te} of turbulent eddies represented by the three horizontal lines at the top of

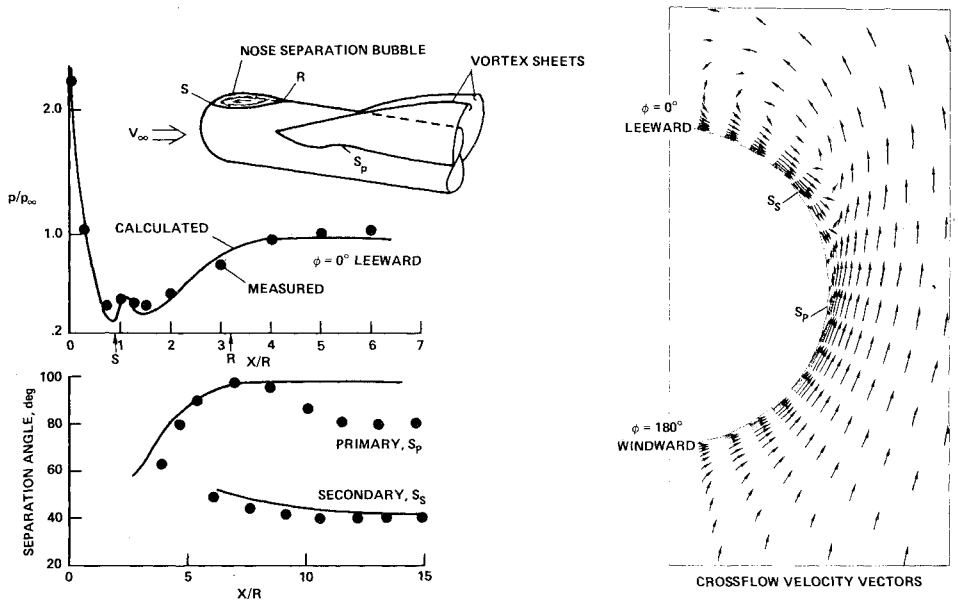

Fig. 12 Computed and measured flow characteristics for an inclined hemisphere-cylinder body; Reynolds aveaged Navier-Stokes computation, $M_\infty = 1.2$, $\alpha = 19$ deg, $Re_D = 445{,}000$, from Pulliam and Lomax (1979).

Fig. 11. The two open circle points in Fig. 11 represent airfoil buffeting[53] and aileron buzz[59] for which frequencies the Reynolds averaged equations have been shown to provide good simulations using the same turbulence models as for steady flow. Being nearly a factor of 100 below f_{te}, the basic concept of Reynolds averaging would be well satisfied in these cases. The solid circle point *CDH* represents the experiments with oscillating turbulent boundary-layer flow of Cousteix, DeSopper, and Houdeville[72] who found that, at the maximum frequency they investigated, the usual steady-flow models of turbulence predicted quite accurately the time-dependent changes in amplitude and phase of the velocity profiles and turbulence intensity. For their test conditions f was only about 0.1 f_{te}. It appears, therefore, that as far as frequency is concerned, many unsteady flows of practical interest are amenable to numerical simulation with the Reynolds averaged Navier-Stokes equations.

It may seem surprising at first that f need be only a factor of 10 below f_{te}. While the average frequency of large-scale eddies passing a given point (x,z) on a surface is f_{te}, the average frequency of eddies passing a given x-station of an airfoil with span equal to one chord length would be the order of $10^2 f_{te}$. For such conditions, Reynolds basic concept for time averaging might be realistic for frequencies f up to the order of f_{te}. On the other hand, for highly three-dimensional flows, with large spanwise variations, f may have to be much smaller than f_{te} to obtain realistic simulations from the Reynolds averaged equations.

A second fundamental question concerns the inherent ability of the Reynolds averaged Navier-Stokes equations to simulate unsteady flows involving broad-band frequency spectra. To date, the successful numerical simulations of unsteady flow—which have been conducted for two-dimensional airfoils without the complications of three-dimensional effects, freestream turbulence, airfoil vibrations or structural oscillations—have yielded an essentially cyclic unsteadiness with a single narrow-band frequency. Experimental flows have many such complexities and involve a broader-band distribution of frequencies. It appears essential to explore computationally the modeling of these complicating phenomena in order to ascertain which ones must be incorporated into Stage III codes in order to simulate unsteady flows with broad-band frequency spectra. Such a simulation capability for the transonic regime has been needed for over two decades and would be of great practical importance. Application could be made, for example, to unsteady inlet flows feeding into compressors, to compressor stall, to certain flutter problems, to gust loads, and to three-dimensional wing buffet that limits transonic maneuverability.

Only in the past year have three-dimensional simulations of turbulent flows been made with the Reynolds averaged Navier-Stokes equations. Because of computer limitations the first such simulation was of the relatively simple three-dimensional flow induced by a swept shock wave interacting with a turbulent boundary layer (Ref. 73). Recently, Shang et al.[74] have computed numerically the flow along a corner for both transitional and fully turbulent flow. Excellent agreement with experiment was obtained for pressure distribution and heat transfer in the former case, and for pressure distribution and surface flow direction in the latter. Pulliam and Lomax[75] use the Stage III approximation to simulate the flow over a hemisphere-cylinder body at angle of attack. This latter case is interesting because it involves three different types of flow separation on the body: a "leading-edge" type separation bubble on the nose, a primary vortex-sheet separation from the sides of the body, and a secondary separation embedded within the primary vortex separation along the upper aft surface. Their results agree quite well with the experiments. An example is shown in Fig. 12. Although the leading edge separation is sketched here as a closed bubble, there is no direct evidence for this since its true three-dimensional shape was not investigated in the computations.

Relative to the inviscid approximations, the Stage III Reynolds averaged Navier-Stokes approximation represents a more youthful stage of development, requires considerably more computer time and memory per case, and consequently is not yet in extensive use by industry. In order to reduce computer time and programming effort, the "thin-layer" approximation to the Navier-Stokes equations has been introduced.[76,77] It accurately resolves viscous stresses in a direction normal to the stream, but not in the streamwise or transverse directions. With the mesh sizes in current use, there is little difference between results from this approximation and from the full Reynolds averaged Navier-Stokes equations.

Turbulence Modeling for Stage III Simulations

As noted earlier, the accuracy of numerical simulations with the Reynolds averaged equations depends principally upon the accuracy of turbulence modeling. Most of the examples of new code developments discussed above used variants of a simple eddy viscosity model. More complex models solve additional differential equations of turbulence

transport simultaneously with the Reynolds averaged equations: 1-equation models solve a differential equation for turbulence kinetic energy; 2-equation models solve two separate differential equations, one for turbulence kinetic energy and one for some other physical quantity such as dissipation or vorticity. The reader interested in specifics is referred to a review by Rubesin[78] and to references sited in the paragraphs which follow. It is noted that turbulence modeling for the Stage III approximation was advanced markedly following MacCormack's development in 1976 of improved numerical algorithms.[79] This reduced the computation time per case from about 10 or 15 h for high Reynolds number flows to about 20 or 30 min, and thereby made practical the investigation of a number of different turbulence models for different flow conditions. Thus most of the information now available on turbulence modeling for the Reynolds averaged equations has been obtained in the past 2 years.

Four different turbulence models have been investigated for the case of separated supersonic flow at high Reynolds number over a compression corner.[51,80] It was found that the simple eddy-viscosity model is reasonably accurate for pressure but not skin friction; the relaxation model of eddy viscosity is very good for pressure, as originally observed by Shang and Hankey,[50] but poor for skin friction; whereas the 1- and 2-equation models are quite good for both quantities. The same four turbulence models yielded essentially the same results for the case of an $M=1.4$ normal shock wave interaction with a turbulent boundary layer over a wide range of Reynolds number, from 9×10^6 to 400×10^6 (Refs. 80, 81). Perhaps it is not surprising that simple 0-equation turbulence models can suffice for pressure distribution which depends largely upon an integral of momentum within a fluid volume, whereas more complex 1- or 2-equation models may be required for skin friction and heat transfer which depend upon a derivative along a boundary of the fluid volume.

Unfortunately, the success of turbulence modeling to date does not extend to hypersonic Mach numbers.[81] None of the four turbulence models were found to be accurate for the case of hypersonic shock-expansion interaction with a turbulent boundary layer. This may be attributed to improper modeling of the very high-density gradients of hypersonic flow and/or the pressure-velocity correlations which are expected to be relatively large in hypersonic flow. Since the latter have thus far proven intractable to measurement even in low-speed flows, there has been no guide as to how such correlations should be modeled. Future computations of turbulence from essentially first principles (Stage IV simulations) may provide a guide.

In view of the fact that investigations of turbulence modeling for the Reynolds averaged Navier-Stokes equations have only been practical for the past 2 or 3 years, the progress to date is significant. Clearly, much additional research is required for three-dimensional flows, hypersonic flows, and for full Reynolds stress models. Although no single "universal" model of turbulence may be found, a limited class of models may be found which applies to representative classes of flows of practical aerodynamic interest.

Stage IV—Turbulent Eddy Simulations

In its full complexity, this stage involves the direct numerical simulation of turbulent eddies from the complete time-dependent Navier-Stokes equations. The main physical concepts are that large eddies extract energy from the mean flow, are highly anisotropic, variable from flow to flow, and transport the principal turbulent momentum and energy; whereas small eddies dissipate energy, tend towards isotropy, are nearly "universal" in character, and transport relatively little turbulent energy or momentum. Thus, the large eddies are computed while the small subgrid scale (SGS) eddies are modeled. Such simulations can be extremely demanding on computer memory and speed. But given sufficient computer power, numerical simulations from essentially first principles could be made of phenomena such as laminar-turbulent transition, aerodynamic noise, surface pressure fluctuations, and all relevant quantities characterizing turbulence. This approach, though now in a relatively primitive research phase, offers tremendous potential for the future. It has already provided some information (e.g., turbulence pressure-velocity correlations) that has long been intractable to experimental measurement. A recent succinct review of large eddy simulation has been outlined by Ferziger.[82]

Many of the pioneering advances in turbulent eddy simulation derive from past research in atmosphere dynamics. Eddy-viscosity and mixing length models, following the ideas of Prandtl and von Kármán, were employed initially in numerical simulations of atmospheric turbulence (e.g., Refs. 83-85). Then in 1963, Smagorinsky[86] described a method of directly simulating large eddies while modeling SGS eddies. Although he used dynamical equations that were not fully three-dimensional, a three-dimensional SGS model for turbulence was developed. The first fully three-dimensional turbulent eddy simulations were made by Deardorff for the flow in a channel[87] and an atmospheric boundary layer.[88] He used a rather coarse grid (6720 mesh points) and modeled both the viscous sublayer and the SGS turbulence.

In turbulent eddy simulations, the smallest resolvable eddies are limited by grid spacing and hence by computer power. Subgrid scale turbulence must be small enough to be modeled without introducing significant uncertainty in the overall turbulence dynamics. Fortunately, experiments indicate that small scales of turbulence approach isotropy, tend to be "universal," and thus can be modeled. Some of the evidence for this derives from measurements of the longitudinal turbulence energy spectral density $E_l(k)$ defined by

$$\int_0^\infty E_l(k)\,\mathrm{d}k=\overline{u'^2}$$

where k is the wave number and u' is the fluctuating velocity at a point. Various spectra, particularly for high Reynolds numbers, are assembled in Fig. 13. Here the dimensionless energy spectra $\Phi=E_l/(\epsilon\nu^5)^{1/4}$ is plotted vs dimensionless wave number k/k_K for eight different types of flow,[89-98] where ϵ is the local rate of energy dissipation per unit mass, ν the kinematic viscosity, and $k_K=(\epsilon/\nu^3)^{1/4}$ is the Kolmogorov wave number related to the Kolmogorov scale η by $k_K=\eta^{-1}$. The Reynolds number R_λ is based on the Taylor microscale λ, velocity $\sqrt{u'^2}$, and ν. For reference, the Kolmogorov scale η corresponds to the lower scales of the dissipating range of eddies: peak dissipation rate, for example, is at $k/k_K\approx0.1$. It is seen that the energy structure of large eddies (small k) vary both with Reynolds number and type of flow, whereas the small, energy-dissipating eddies (large k) are apparently universal—e.g., independent of both Reynolds number and type of flow. The small eddy spectra agree well with the theory of Pao.[99] Thus there is sound experimental foundation for large eddy simulation; that is, for numerically simulating the anisotropic, Reynolds-number, and flow-dependent large eddies, while modeling the small subgrid scale eddies that are universal and tend toward isotropy. The modeled eddies would be nonisotropic but with small shear.

Various types of turbulent eddy simulations have been made: some model subgrid scale turbulence, others do not; some model the near-wall regions, others do not; and some use the inviscid Eulerian equations for computing outer eddy dynamics, while others use the Navier-Stokes equations. As yet there is no common terminology for the various types. In this paper the generic term "turbulent eddy simulation" encompasses all types, while "large eddy simulation" (LES) refers to methods that model the subgrid scale turbulence and in some cases also model the small-scale turbulence in the viscous sublayer. Vortex dynamic simulations (Refs. 100 and

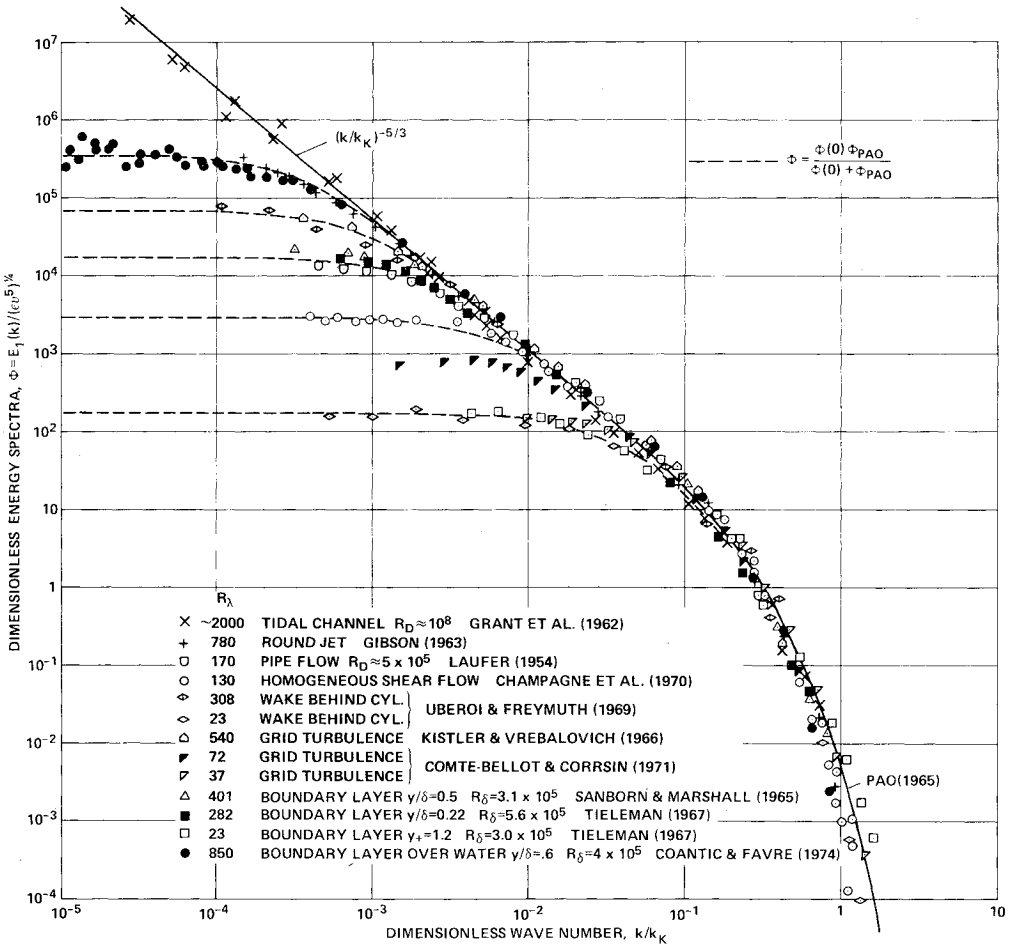

Fig. 13 Streamwise turbulence energy spectra for various flows.

101) can be viewed as a type of turbulent eddy simulation that uses discrete vortices as a coarse form of turbulence computation and that may or may not involve modeling of turbulence fine structure.

The simplest case of homogeneous isotropic turbulence has received considerable attention. With the use of spectral methods for efficient computation, Orzag and Patterson[102] conducted numerical simulations using a 32^3 grid. Thus far, spectral methods have been limited to incompressible fluids and to flows with simple geometric boundary conditions. The calculations of Fox and Lilly,[103] also using a 32^3 grid system, illustrate clearly the major difference between two- and three-dimensional turbulence: energy cascades upscale to larger eddies in two-dimensional, and downscale to smaller eddies in three-dimensional. More refined computations using a 64^3 grid system have been made recently by Clark et al.[104] and Rogallo.[105] These latter computations provide a base for testing subgrid-scale turbulence models with coarser meshes and can be applied to homogeneous shear-flow turbulence.

Channel flow has also received considerable attention. Following Deardorff's work, Schumann[106] used a finer grid system (up to 65,536 points) and a refined SGS turbulence model. He divided the SGS turbulence into an inhomogeneous part and a locally isotropic part and employed a separate dynamic equation ("1-equation" model) for the transport of turbulent energy. Grötzbach and Schumann[107] extended the code to account for temperature fluctuations and heat transfer. In most respects, the numerical simulations agree with experiments as well as various experiments agree with each other. All of these computations model both the SGS turbulence and the viscous sublayer turbulence (the latter by a law of the wall). The first large eddy simulation of channel flow that computed rather than modeled viscous sublayer turbulence was that of Moin et al.[108] In agreement with experiment, their numerical computations revealed a turbulence structure of ejection events ($u'<0$, $v'>0$) and sweep events ($u'>0$, $v'<0$) within a three-dimensional sublayer of high activity containing streamwise elongated vortices alternating spanwise with low and high velocity. Because of the relatively coarse grid (16,640 points, $\Delta z_+ = 168$), the computed sublayer structure was fatter than experiment, and the longitudinal vortices were separated spanwise considerably more than the experimental mean spacing of 100 wall units. The computed wall-pressure fluctuations agreed well with experiment, as did $\overline{u'^2}$ and $\overline{w'^2}$, but the agreement of $\overline{v'^2}$ was only fair, due perhaps to the particular SGS model used in combination with a highly elongated grid volume.

Turbulent eddy simulations also have been made for free shear layers and wakes. Mansour et al.[109] simulated the time-evolving one-dimensional free shear layer. They observed that vortex structures paired even in a background of considerable turbulence and that the shear layer development depends on the initial disturbance field. Both of these results are compatible with experimental observations. Limited computations of the turbulent flow in an axisymmetric momentumless wake have also been made.[110]

Whereas all of the above simulations are for incompressible flow, Wray[111] has recently conducted turbulent eddy simulations for compressible flow in free shear layers and round jets. He used different types of initial disturbance for each type of flow. His numerical computations of a two-dimensional free-shear layer, illustrated in Fig. 14 as vorticity contours, clearly show the vortex pairing phenomenon observed experimentally (Ref. 112). Interestingly, a three-dimensional initial disturbance in the shear layer did not result in the large-scale pairing vortex structure, but developed into the more common irregular three-dimensional turbulence structure (Fig. 15). Such results also are compatible with

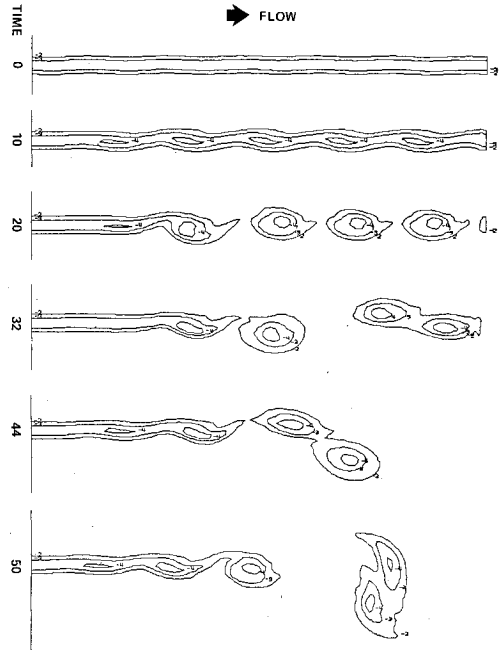

Fig. 14 Numerical computation of free-shear layer with two-dimensional initial perturbation; $M=0.5$, Navier-Stokes turbulent eddy simulation, unpublished results of Wray (1978).

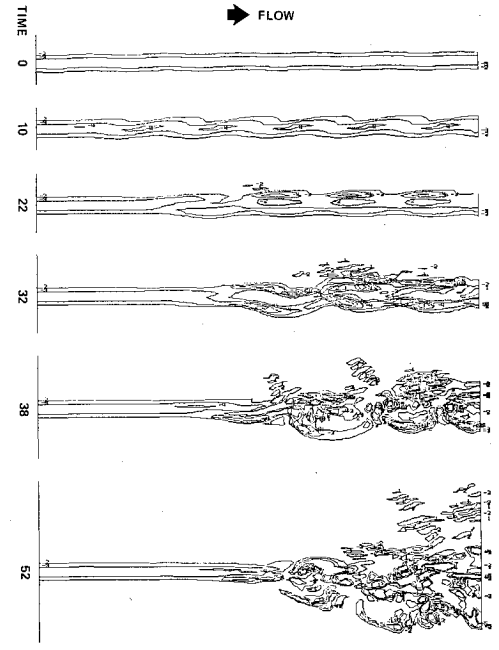

Fig. 15 Numerical computation of free shear layer with three-dimensional perturbation; $M=0.5$, Navier-Stokes turbulent eddy simulation, unpublished results of Wray (1978).

experiments (Ref. 113). One of Wray's simulations of the three-dimensional turbulence in a nearly round jet is illustrated in Fig. 16. From simulations of this nature, the details of aerodynamic noise generation, for example, can be explored, as can many aspects of turbulence dynamics. It is this writer's opinion that in the long run, with much more powerful computers of future decades, large eddy simulation will become a practical tool for accurate, detailed, fluid-dynamic simulations in many different fields of engineering. It will also become a valuable research technique for understanding certain aspects of turbulence.

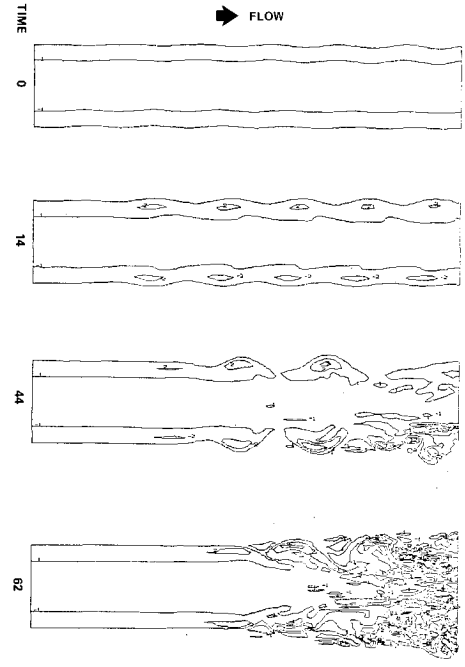

Fig. 16 Numerical computation of flow in round jet with nonaxially symmetric initial perturbation; $M=0.5$, Navier-Stokes turbulent eddy simulation, unpublished results of Wray (1978).

Future Computer Requirements

Reynolds Averaged Simulations

In making estimates of future computer requirements, attention is focused on the grid point requirement which translates directly into computer memory requirement. Computing time with the Reynolds averaged equations is roughly proportional to the number of grid points N and, for a given N, is nearly independent of Re (Refs. 44 and 73). This independence arises because the effective eddy viscosity is proportional to $U_e\delta$ and increases with Re, leaving the mesh Reynolds number nearly independent of Re. Since numerical algorithm efficiency improves with time, the future improvement factors required for computer memory using the Reynolds averaged equations will be greater than for computer speed. Consequently, emphasis in the discussion which follows is placed on grid point requirements.

The primary variable determining the required number of grid points is the boundary-layer thickness δ. Let n_x, n_y, and n_z be the average number of grid points per length δ in the directions x (streamwise), y (across boundary layer), and z (spanwise), respectively; let $\bar{\delta}$ be the average boundary-layer thickness, so that the average grid point spacings $\overline{\Delta x}$, $\overline{\Delta y}$, and $\overline{\Delta z}$ are $\bar{\delta}/n_x$, $\bar{\delta}/n_y$ and, $\bar{\delta}/n_z$, respectively. Thus, the product $n_x n_y n_z$ represents the average number of grid points in a volume $\bar{\delta}^3$. Further, let N_x, N_y, and N_z be the number of grid points in the boundary layer along the chord, across the layer, and along the span, respectively. The well-known simple equations for boundary-layer thickness on a flat plate of chord c

$$\delta/c=0.37\ Re_c^{-0.2} \qquad \bar{\delta}\approx 0.6\delta \tag{1}$$

will be used to estimate $\bar{\delta}$, recognizing that in favorable gradients $\bar{\delta}$ will be smaller and in adverse gradients larger. Then, for a wing of span b and aspect ratio $\mathcal{R}$,

$$N_x=\frac{c}{\overline{\Delta x}}=\frac{c}{\delta_c}\frac{\delta_c}{\bar{\delta}}\frac{\bar{\delta}}{\overline{\Delta x}}=4.5n_x Re_c^{0.2} \tag{2}$$

$$N_y=c/\overline{\Delta y}=n_y \tag{3}$$

$$N_z = \frac{b}{\overline{\Delta z}} = \frac{b}{c}\frac{c}{\delta_c}\frac{\delta_c}{\bar{\delta}}\frac{\bar{\delta}}{\overline{\Delta z}} = 4.5 \mathcal{R} n_z Re_c^{0.2} \tag{4}$$

and the total number of grid points within the wing boundary layer becomes

$$(N_w)_{BL} = 0.4\ \mathcal{R}\ n_x n_y n_z Re_c^{0.4} \times 10^2 \tag{5}$$

For other portions of the flowfield, estimates based on current experience will be used of $(1/2)N_{BL}$ for the number of grid points in the viscous wake, and 2×10^5 points for the outer inviscid field. In making estimates of the number of grid points, the value $n_x n_y n_z = 10$ will be used, corresponding, for example, to $n_x = 1$, $n_y = 20$, $n_z = 0.5$, i.e., to an average streamwise grid spacing of $\bar{\delta}$, to 20 points across the layer, and to an average spanwise spacing of $2\bar{\delta}$. This represents a finer overall resolution than is currently used (e.g., Refs. 53, 55, and 59) of $n_x = 0.3$ to 0.7, $n_y = 18$ to 25, and $n_z = 0.3$ (Kordulla[114]) corresponding to values of $n_x n_y n_z$ between 2 and 5. Adding the various component requirements together and using $\mathcal{R} = 4$, the estimates in Table 2 are obtained for total number of grid points N_w and for computer memory.

In Table 2 the requirement of about 30 words of memory per grid point is used, an approximate value for Reynolds averaged simulations that employ a complex turbulence model. For compressor and turbine blades with $1 < \mathcal{R} < 6$ operating at representative Reynolds numbers in the range from 0.3×10^6 to 3×10^6, the estimated grid point requirements for different blades vary between 3×10^5 and 8×10^5. Also, for an $\mathcal{R} = 12$ helicopter rotor blade operating at an average Re of several million, about 4×10^6 grid points would be required.

Similar estimates can be obtained for Reynolds averaged simulations of the flow over a fuselage or a body at angle of attack. Using the same simple approximation in Eq. (1) for δ and defining πD as the average circumference of a body of length L, we obtain for the number of grid points in the body boundary layer $(N_B)_{BL} = 64(D/L)Re_L^{.4} n_x n_y n_z$. For a body of $L/D = 5$, this is about 1/6 to 1/7 the number of points for an $\mathcal{R} = 4$ wing. Again, assuming $(N_B)_{\text{wake}} = (1/2)(N_B)_{BL}$ and taking $N_{\text{inv}} = 10^5$ for the inviscid outer flow, the estimates in Table 3 are obtained for the total number of grid points N_B. This estimate corresponds to considerably finer resolution than used in existing simulations (e.g., $N_B = 2\times10^4$ in Ref. 75) which employ a coarser mesh than desired because of computer memory limitations.

Rough estimates can also be made for a representative aircraft in the cruise condition. Assuming that the number of grid points for the tail surfaces N_T is half that for the wing, that the number for nacelles and pylons N_N is three times that for the fuselage, and using $L/D = 5$ and $L/c = 5$, we obtain the order of magnitude estimates shown in Table 4. In these estimates it is presumed, of course, that nested grid systems with appropriate grid spacing would be used for each configuration component. If the wing aspect ratio is higher/lower than assumed ($\mathcal{R} = 4$), the corresponding values for $N_{A/C}$ would be higher/lower.

Table 2 Wing, $\mathcal{R} = 4$, Reynolds averaged

Re_c	10^6	10^7	10^8
N_w	8×10^5	2×10^6	4×10^6
Memory (words)	2×10^7	6×10^7	10^8

Table 3 Body at α, $L/D = 5$, Reynolds averaged

Re_L	10^6	10^7	10^8
N_B	1.5×10^5	2×10^5	4×10^5
Memory (words)	5×10^6	6×10^6	10^7

Turbulent Eddy Simulations

Past estimates of the grid point requirements for conducting turbulent eddy simulations with the Navier-Stokes equations have indicated immense numbers for N. This has led to gloomy conclusions as to the practicality of such simulations in the foreseeable future. It is this writer's view that such estimates have been based on unnecessarily restrictive assumptions, and have led to misleading conclusions. Consequently, the paragraphs which follow go into some depth in order to form more realistic estimates of the grid point requirements for turbulent eddy simulation.

In making past estimates, one approach has been to assume that the required mesh spacing Δ must resolve the dissipation eddies, and hence correspond to a "Kolmogorov grid," for which, $\Delta = \eta = (\nu^3/\epsilon)^{1/4}$. Since a minimum of 5 to 6 points is required to resolve a wave length λ, where $\lambda = 2\pi/k$, this assumption corresponds to numerical resolution up to dimensionless wave numbers $k/k_K \approx 1$, and to direct computation of virtually all of the small dissipating eddies, even though at high Reynolds numbers the fraction of turbulent energy and shear in these eddies is trivially small. Following Rubesin,[78] the overall volume average $\bar{\eta}_v$ of the Kolmogorov microscale upstream of station x on a flat plate is computed from the equation relating energy dissipated to drag times velocity,

$$n_v = \frac{1.5x}{Re_x^{3/4}} = \frac{2.05\delta}{R_\delta^{.688}} \qquad \bar{\eta}_p = 1.25\bar{\eta}_v \tag{6}$$

where $\bar{\eta}_p$ is the profile average of η across the boundary layer. A Kolmogorov grid throughout a given volume leads to $N \sim Re^{9/4}$ (Ref. 115), and throughout a boundary layer of thickness varying with Re, leads to $N \sim Re^{41/20}$ (Ref. 78). Estimated values of N for examples of interest are extremely large, on the order of 10^{13} and higher (Refs. 78, 115, and 116). An alternate approach of Emmons[117] was to assume that the small scales of turbulence important near a wall define the required griding throughout the entire turbulent region. This also leads to extremely large values of N.

Serious objections are raised to approaches such as the above which assume that either the Kolmogorov grid scale, or some other very small grid scale, demonstrably required in the viscous sublayer, must also be used throughout the entire turbulent region. At high Re such small scales represent an important part of the momentum and energy balance only in a very thin dissipative layer near the wall. Also Kolmogorov scaling requires that as Re is increased, an increasingly large fraction of the total turbulent kinetic energy must be directly computed, rather than a constant fraction for all Re. Consequently, in the paragraphs which follow new estimates are made of the grid point requirements for turbulent eddy simulations using available experimental information on the relative amounts of energy and shear in various scales of turbulent motion.

The longitudinal turbulent energy spectra presented in Fig. 13 cover a wide range of Re and form a basis for estimates of grid requirements. The dashed curves in this figure, representing the empirical function $\Phi = \Phi(0)\Phi_{Pa0}/(\Phi(0) + \Phi_{Pa0})$, approximate the spectra. Since Φ_{Pa0} is an analytical function,[99] integrations can readily be made to yield the fraction R of kinetic energy contained in wave

Table 4 Wing-body-tail-nacelles, Reynolds averaged

Re_c	10^6	10^7	10^8
$N_{A/C}$	2×10^6	4×10^6	9×10^6
Memory (words)	6×10^7	10^8	3×10^8

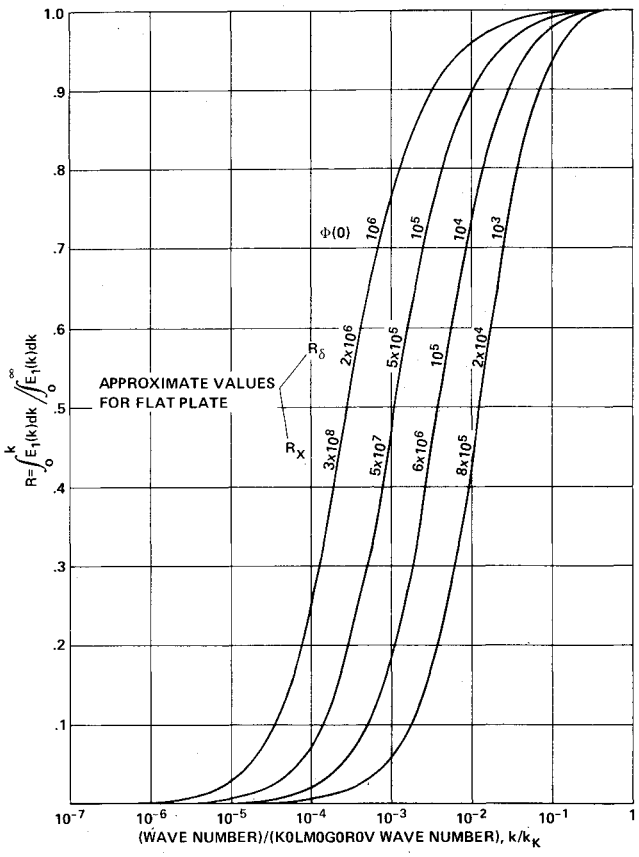

Fig. 17 Fraction of turbulent kinetic energy in wave numbers below a given value of dimensionless wave number, k/k_K.

numbers up to k

$$R=\int_0^k \Phi(k)\,dk \Big/ \int_0^\infty \Phi(k)\,dk \tag{7}$$

Figure 17 shows a plot of R vs k/k_K for various values of $\Phi(0)$. Each value for the dimensionless intercept $\Phi(0)$ of the spectra corresponds to a particular value for the entire integral

$$g(\infty)=\int_0^\infty \Phi\, d(k/k_K)$$

namely $g(\infty)=18.8$, 52.7, 139, and 356 for $\Phi(0)=10^3$, 10^4, 10^5, and 10^6, respectively. Approximate values of Re for the outer turbulent region of the boundary layer on a flat plate can be assigned to each $\Phi(0)$. By using Eq. (1),

$$g(\infty)=\int_0^\infty \Phi\, d(k/k_K)=\frac{\overline{u'^2}}{\nu^2 k_K^2}$$

$$\equiv \frac{\overline{u'^2}}{U_e^2}\left(\frac{\eta}{\delta}\right)^2 Re_\delta^2=\left[\frac{\sqrt{\overline{u'^2}}\,\eta}{U_e\eta_p}\right]^2 \frac{Re_\delta^{1/2}}{(u_*/U_e)} \tag{8}$$

Because $\sqrt{\overline{u'^2}}$ decreases while η increases with y across the outer turbulent region, the quantity in square brackets does not vary greatly across a flat plate boundary layer, being, for example, 0.095 ± 0.02 for $0.01<y/\delta<0.8$ according to the measurements of Klebanoff.[118] This makes it possible to relate a very appropriate value of Re_δ, and hence Re_x, for the outer turbulent region of a flat plate to each value of $\Phi(0)$ or $g(\infty)$, as indicated in Fig. 17. These approximate values would not apply to the viscous sublayer region.

Several significant points follow from the results of Fig. 17. First, if all turbulent eddies were computed up to a wave

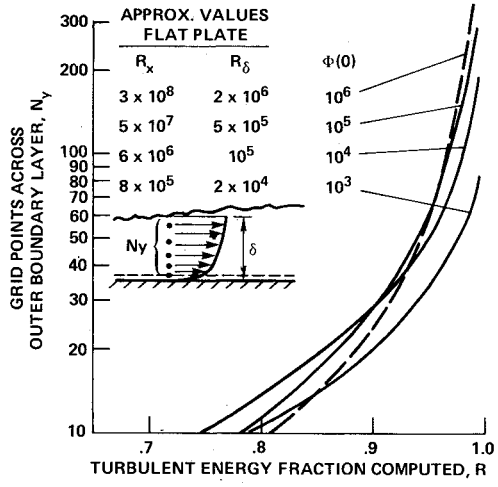

Fig. 18 Required number of grid points across turbulent layer in region external to viscous sublayer.

number $k/k_K=1$, the ratio R of computed to total turbulent energy would increase with Reynolds number, amounting, for example, to 0.99995 at $R_\delta\approx 2\times10^4$, and 0.999998 at $R_\delta\approx 2\times10^6$. Such values of R are much closer to unity than required for practical computations. Also, a more realistic criteria would be $R=$ const independent of Reynolds number. Figure 18 shows that if a constant value of R is selected, e.g., $R=0.9$ with the remaining 0.1 fraction of turbulent energy modeled, then the required grid spacing is essentially independent of Re. The curves in Fig. 18 derive from those of Fig. 17 together with the relationship for wave length $\lambda=2\pi/k$ and the assumption $\Delta y=\lambda/5$ of 5 grid points minimum to resolve a wave. For $R=0.9$ it is seen that 20 to 28 grid points would be required across the outer turbulent layer. Independent experiments corroborate this result: the shear spectra of Ramaprian and Shiraprasad,[119] for example, show that resolution of 0.9 of the turbulent shear requires $k\delta=20$, or $\pi\delta=10\lambda$, which, with $\Delta y=\lambda/5$, requires $\delta/\Delta y=16$ grid points across the boundary layer. Similarly, integration of the shear spectra of Klebanoff[118] also yields a value of about $n_y=16$ points for $R=0.9$. Measurements of Bradshaw[120] indicate that the dimensionless energy and shear spectra, especially for the smaller scales of turbulence, are not greatly affected by moderate pressure gradients. In consideration of the overall data, a value $n_y=25$ is used in subsequent calculations for all Re. This corresponds to modeling subgrid scale turbulence that is nonisotropic with small-shear transport and is within the universal range.

It is emphasized that the preceding result for turbulent eddy simulations of essentially Reynolds-number independence for the number of grid points across an outer turbulent region (exterior to the viscous sublayer) differs from previous analyses which have indicated a strong dependence on Reynolds number.

A simple physical interpretation of the preceding results can be given. Coherent turbulence structures for the outer turbulent region scale with δ. As Re increases, the turbulence energy absorbed from the mean flow cascades farther downscale to reach eddy sizes that can dissipate energy. Once the scales reach a certain fraction of δ—and long before they reach the very small dissipative scales in a high Re flow—almost all of the turbulent energy and shear are accounted for. Thus the momentum and energy equations in the outer region can be balanced accurately at high Re with only an approximate modeling of the small dissipating eddies. In the viscous sublayer, however, the dissipation eddies are an important part of the energy balance and momentum transport.

Direct computation of 90% of the turbulent kinetic energy, for example, with the remaining 10% of small-scale energy

modeled, should not result in significant uncertainties due to modeling. For flows with modest amounts of separation, the entire large- and small-scale turbulence transport of energy and shear can usually be modeled to an accuracy better than an order of 10-20%. The uncertainty in modeling the more universal small-scale turbulence should be less, perhaps 5-10%. This would yield an overall uncertainty due to subgrid scale modeling of only 0.5-1%, quite acceptable for practical engineering.

In making estimates of LES grid point requirements, a value of $n_x n_y n_z = 2500$ is used for the turbulent regions exterior to the viscous sublayer. This would correspond, for example, to $n_x = 10$, $n_y = 25$, $n_z = 10$; e.g., to 25 points across the outer part of the boundary layer, to $\Delta x = 2.5\,\Delta y$ in accordance with the average proportions of typical eddy structures,[121-123] and to $\Delta z = \Delta x = \delta/10$. In the turbulent eddy simulations made to date for channel flow, values of $n_x n_y n_z$ between 312 and 1024 have been used.[87,106,108] Hence the value 2500 grid points per δ^3 would correspond to a finer resolution of the turbulent eddies than realized in these existing simulations.

Estimates will be made first for large eddy simulations in which both the subgrid scale turbulence and the viscous sublayer turbulence are modeled. It is to be noted that at high Re the "outer" portion extends over about 99% or more of the overall turbulent layer thickness. For an airfoil, computations of three-dimensional turbulence over a constant-chord wing of span about $c/5$ would be sufficient to avoid transverse contamination effects of using periodic boundary conditions at the span edges. If we take $N_{\text{wake}} = (1/2)N_{BL}$, as before, then Eq. (5) applies with a value of $n_x n_y n_z = 2500$ and $\mathcal{R} = 1/5$. The estimated grid point and memory requirements for an airfoil are given in Table 5. The estimate of memory assumes that in the outer turbulent region where laminar shear is negligible compared to turbulent shear, it would be adequate to use the Eulerian equations which only require 15 words storage or less per grid point. Similar estimates of N_w and memory for a wing of $\mathcal{R} = 4$ are 20 times the values in Table 5. Using the equations derived earlier for a body at angle of attack, values are obtained for N_B of about 1.5 times the corresponding values above for N_A.

The corresponding estimates for a wing body would be about 1/2 the numbers estimated in Table 6 for a reasonably complete aircraft of wing, body, tail, nacelles (again assuming $N_T = N_w/2$, and $N_N = 3N_B$).

In regard to requirements on computer speed for LES, it is noted that the above analysis yields a grid spacing Δx that scales with δ. Computing time increments Δt would vary with Δx, so that the computing time per grid point would vary weakly with Re (as the 0.2 power) and would only be about two and one-half times as great, for example, at $Re = 10^8$ as at $Re = 10^6$. Computing time for LES in the outer turbulent region, therefore, will depend mainly on the number of grid points.

We turn now to estimates for turbulent eddy simulation of the extremely small physical scales of viscous sublayer dynamics. These scales increase with distance y from the wall.

Table 5 Airfoil, LES

Re_c	10^6	10^7	10^8
N_A	8×10^6	2×10^7	5×10^7
Memory (words)	10^8	3×10^8	8×10^8

Table 6 Aircraft, LES

Re_c	10^6	10^7	10^8
$N_{A/C}$	3×10^8	8×10^8	2×10^9
Memory (words)	3×10^9	10^{10}	3×10^{10}

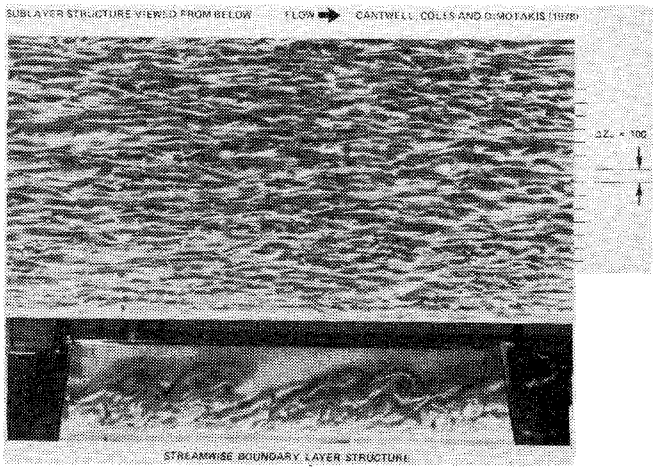

Fig. 19 Flow visualization of sublayer structure and streamwise boundary-layer structure; from Cantwell et al. (1978).

In the laminar sublayer ($y_+ < 15$), the structures are highly elongated,[124-127] as shown in Fig. 19 from Cantwell et al.[127] As illustrated, the longitudinal structures are spaced about 100 wall units apart, for which a spanwise grid spacing near the wall of $\Delta z_{+w} \approx 20$ or less might be required for adequate resolution. Clark and Markland[125] indicate that in the region out to about $y_+ = 70$, the average streamwise length of the structures is $\ell_{+x} \approx 440$, for which $\Delta x_{+w} \approx 100$ would be required. It is emphasized that the viscous sublayer is very thin, extending roughly to $y_+ \approx 100$ and is about 1% of the boundary-layer thickness at Re_x of aerodynamic interest. Generally, this is only a few tenths of a millimeter, considerably less than the skin thickness of an aircraft. The dynamics in such thin regions adjacent to a wall are anticipated to be universal functions of local wall conditions.

The efficient computational resolution of viscous sublayer dynamics would require using nested grids with mesh spacing increasing with distance from the wall. The Δy spacing would be highly nonuniform ranging from $\Delta y_+ \approx 1$-2 for the first point from the wall (less than the Kolmogorov length η_{+w} of 2-4) to $\Delta y = \delta/25$ in the outer turbulent region. It is assumed that multiple blocks of nested grids would be used with each block containing on the order of 10 layers of grid points of constant Δx and Δz spacing, and with Δx and/or Δz doubling outward from block to block to reach values compatible with the grid spacings in the outer turbulent region. With Δx and Δz doubling across blocks, each block would contain about 4 times the number of grid points in the block above. To quantify this type of nested grid, consider a small element ΔA of surface area ℓ_x by ℓ_y, and let n_{yl} be the number of y-direction grid points in the first block next to the surface which contains most of the grid points ΔN_{vs} in the viscous sublayer above ΔA. We have

$$\Delta N_{\text{vs}} \approx \frac{4}{3}\frac{\ell_x \ell_y n_{yl}}{\Delta x_w \Delta y_w} = \frac{4}{3}\frac{n_{yl}}{(\Delta x_{+w})(\Delta z_{+w})}\frac{\tau_w \Delta A}{\rho_\infty \nu^2} \tag{9}$$

Since the average skin friction coefficient is $C_F \rho_\infty U_\infty^2 S = 2\int \tau_w dA$, where S is the wetted surface area of integration, the total number of grid points in the viscous sublayer is

$$N_{\text{vs}} \approx \frac{2}{3}\frac{n_{yl} C_F S Re_c^2}{(\Delta x_{+w})(\Delta z_{+w}) c^2} \tag{10}$$

Using the simple flat plate equation $C_F = 0.074\, Re_L^{-0.2}$ there results

$$N_{\text{vs}} \approx 0.05\frac{n_{yl} S Re_c^{1.8}}{(\Delta x_{+w})(\Delta z_{+w}) c^2} \tag{11}$$

This dependence on Re is much greater than the $Re^{0.4}$ dependence for turbulent eddy simulations in which the viscous sublayer is modeled. The simple dependence on S simplifies estimates for complex configurations.

For estimates we take $n_{yl} = 10$, and $(\Delta x_{+w})(\Delta z_{+w}) = 2000$ (e.g., $\Delta z_{+w} = 20$, $\Delta x_{+w} = 100$), so that $N_{vs} = 2.5\,(S/c^2)\,Re_c^{1.8} \times 10^{-4}$. This number is so large for Re of interest that the number of grid points in the outer turbulent region can be disregarded (except at lower Re near 10^6), and the number in the inviscid region would be negligible. For an airfoil, $S/c^2 \approx 0.4$, and the combined number of grid points for viscous sublayer and outer turbulent layer is given in Table 7. In Table 7 25 words storage per grid point is used, an approximate value for the full Navier-Stokes equations with a modest SGS model. Equation (11) can also be used to estimate the approximate number of grid points required to compute transition and the development of a turbulent spot. The experiments of Cantwell et al. show the structure under a spot to be of the same small scale as under a turbulent layer. Assuming that transition and spot development occur over the downstream half of the computational domain, we obtain $N_{\text{transition}} \approx 3 \times 10^6$ for $Re = 10^6$, and memory $\approx 8 \times 10^7$ words. For the case of a complex aircraft the wetted area would be of the order of $S/c^2 = 20$, resulting in the order of magnitude estimates of Table 8.

The estimates in Table 8 presume that for each flow the viscous sublayer dynamics extremely close to a wall need be resolved down to very small scales. It would be preferable to treat such dynamics as universal, represented by a generalized three-dimensional law of the wall. Such a law would have to embody whatever aspects of time-dependent dynamics that are essential for providing a lower boundary condition for the outer turbulent region. If, as suggested by Landahl,[128] for example, the outer large-scale turbulence is driven by Reynolds stress dynamics of the small scales, then the essential aspects of such dynamics would be part of the general boundary condition. Development of such a law, either computationally or experimentally, would make it unnecessary to compute the fine structure of viscous sublayer dynamics for each and every flow, and the grid-point requirements would be reduced to those estimated earlier for LES.

Outlook for Future Computer Capability

It is essential to recognize at the outset that the computer market environment in the past decade has undergone a major revolution undermining the economic incentives to develop new scientific supercomputers. During the initial years of electronic computing, the main drivers were defense interests, and the federal government owned all computers; now the main drivers are consumer interests (e.g., digital watches, calculators, TV games, business minicomputers, toys, CB radio, etc.), and the private sector owns 97% of the computers. Through the mid-1960's, supercomputers formed nearly 100% of the market; now they form only a small percentage and are projected to form a trivial percentage in the future (Ref. 129). Through the 1960's, the technology drivers were for fast circuits in large computers time-shared by many users; now they are for more memory in small computers distributed to each user. Whereas computers were used through the 1960's mainly as numerical calculating engines, they now are used mainly for information processing. Whereas forceful sponsorship for supercomputer development was provided by the federal government in the late 1940's and early 1950's and by major private capital through the 1960's, there now is no such driving sponsorship in the U.S. The net result of these changes is that, in contrast to earlier decades, supercomputers no longer are a focus for the development of new component technology, and no significant economic incentive exists for corporations to risk major capital in the development of advanced supercomputers. Some have concluded (Ref. 130) that maintenance by the U.S. of world leadership in scientific computations will require that the federal government resume its earler policy of providing substantial funds for the development of advanced supercomputers.

The computer market revolution has also affected concepts about the architecture of large computers. As stated by Best,[129] supercomputers of the future can attain their goals only by exploiting all levels of parallelism with a computer structure assembled from conventional componets developed for other end-user requirements (i.e., the mass market). This view, in the present writer's experience, is widely held by computer architects of the major large-computer companies. Partly in recognition of these circumstances, the Ames Research Center has been planning and advocating for several years that NASA undertake the development of a Numerical Aerodynamic Simulation Facility (NASF). Such a facility would provide a major new computational capability for aerodynamics, and could be a pathfinder for other scientific computers to follow. To date, feasibility and preliminary design studies have been conducted and points identified as "NASF" in various figures are based on these studies (Refs. 131 and 132).

In projecting future capabilities of large computers, an assessment will be made first of memory, then of speed. Fortunately, consumer demand for more memory appears nearly insatiable and the mass market for memory essentially elastic.[133,134] As a result, memory is the most rapidly advancing technology in microelectronics. Thus the future prospects for larger, more cost-effective memories are bright. Figure 20 illustrates the past trends in chip density for bipolar ECL, dynamic MOS, and CCD memory. The future projections, shown by short dashed lines, are those of semiconductor chip manufacturers (Refs. 134-136). A recent projection of Hammer[137] is considerably more optimistic than those shown in Fig. 20. The rate of growth of bipolar-

Table 7 Airfoil, LES with sublayer resolution

Re	10^6	10^7	10^8
N_A	1.4×10^7	4×10^8	2×10^{10}
Memory (words)	4×10^8	10^{10}	5×10^{11}

Table 8 Aircraft, LES with sublayer resolution

Re_c	10^6	10^7	10^8
$N_{A/C}$	3×10^8	2×10^{10}	10^{12}
Memory (words)	8×10^9	5×10^{11}	3×10^{13}

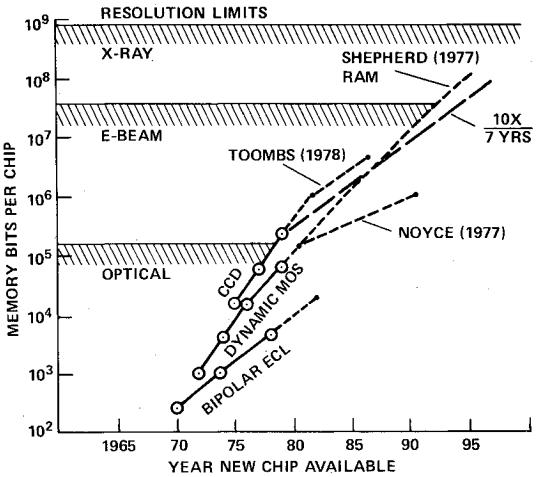

Fig. 20 Trends in bit density of semiconductor memory chips.

ECL, the fastest memory, has been considerably smaller than for MOS memory probably because of the smaller market for high-speed memory. The cost-reduction trend for memory is approximately a factor of 10 each 7 years (Refs. 138 and 139), essentially the same as the cost-reduction trend for a given amount of numerical computation (Fig. 1). Thus a factor of 10 change in 7 or 8 years has been an average trend of "computer efficiency improvement." Such a trend is shown in Fig. 20 as a long dashed line projecting from the point corresponding to a 256-K CCD chip in 1979. It does not differ greatly from the projections of Shepherd[135] or Toombs[136] and will be used as a reference line in subsequent figures. Since the cost of production chips changes relatively little with packing density, the projections of Toombs and Shepherd would correspond roughly to projections of future memory increase for essentially constant cost. The physical resolution limits shown for optical, E-beam, and x-ray lithography indicate room for sufficient future growth without encountering any fundamental lithographic limit in this century (Refs. 135 and 140).

Projections of chip density, and considerations of cost, form the principal basis for estimating future computer memory capacity. The past history and projected future of large-computer memory are shown in Fig. 21. Following rapid early growth of electrostatic and electromechanical devices, the faster ferrite core memory was used for over 15 years until supplanted by the still faster semiconductor technology. Memory capacity dropped with the introduction of ECL and MOS because of much shorter access time and similarly will jump with the introduction of CCD staging memories having longer access times than ECL or MOS. The first known computer to employ a CCD backup memory is the Burroughs Scientific Processor (BSP). The preliminary designs for NASF involve a large CCD memory, up to 2.6×10^8 words, to meet the large grid-point requirements of computational aerodynamics. Future expectation, based on the chip density projection of Fig. 20, is that memories of 10^{10} to 10^{11} words, for example, could be available in the 1990's. This is believed to be a realistic estimate for roughly constant memory cost. Since NASF represents a relatively large computational facility, the dashed-line projections would correspond to feasible memory for such computers.

It is to be noted that throughout this paper the projections of future computer capability (such as indicated in Fig. 21 by the points NASF and BSP through which dashed lines extend) represent estimates for what currently appears to be technically feasible in the future. What actually is attained may be different since a number of other factors such as future changes in market opportunities, funding limitations, national security concerns, unanticipated technical problems and technical breakthroughs can also bear importantly on the capability of future large-scale scientific computers.

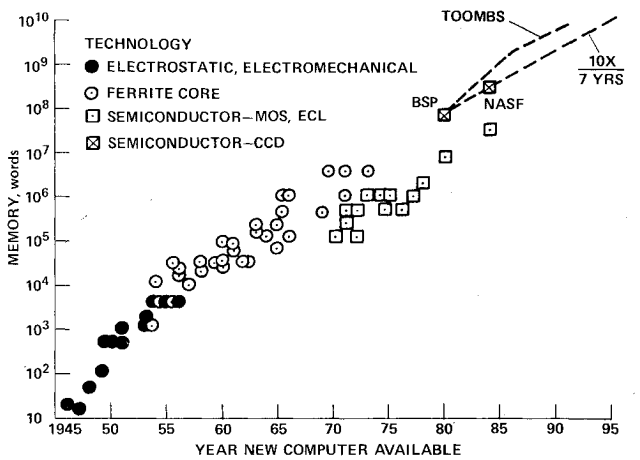

Fig. 21 Development trend of main memory for large computers.

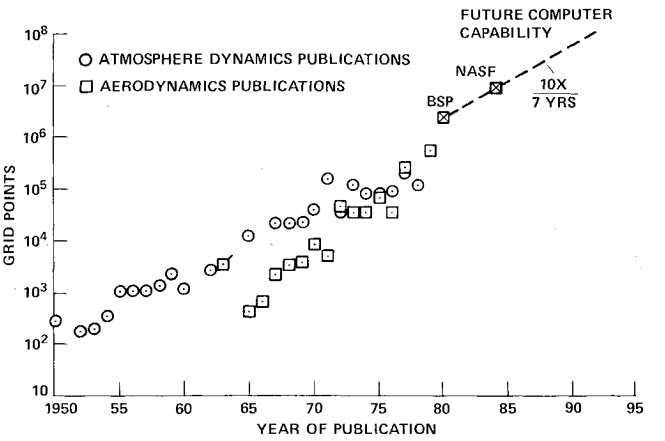

Fig. 22 Growth in maximum number of grid points used in computational fluid dynamics publications.

Computer memory capacity translates nearly directly into grid-point capability. From a perusal of various publications on atmosphere dynamics (mainly on global circulation models) and on aerodynamics, a plot has been made in Fig. 22 of the maximum number of grid points employed in various years of publication in these two fields. The initial point for 1950 corresponds to the first numerical weather prediction, which was conducted on the ENIAC computer by Charney, Fjörtoft, and von Neumann.[141] They used only 270 grid points (15×18) to cover the Northeastern Pacific, North America, and Northwestern Atlantic. The last point plotted for 1979 corresponds to the turbulent eddy simulations of Wray[111] (Figs. 15 and 16) who used 500,000 grid points on the ILLIAC IV. The largest available computers have always been employed for numerical atmosphere dynamics, and it is clear from Fig. 22 that aerodynamicists did not catch up until about 1975. The single-tagged square point for 1963 represents the pioneering work of Fromm and Harlow[142] in simulating the vortex street behind a plate. They were then with the Atomic Energy Commission, an agency that consistently has had the most powerful available computers to work with. Over the decades following ENIAC, the increase in grid-point capability has been somewhat less than the increase in memory, since the use of progressively more refined approximations to the governing equations requires more words of memory per grid point. The dashed reference line in Fig. 22 corresponds to the average rate of computer efficiency improvement, and to a storage requirement of 30 words per grid point appropriate for Reynolds averaged simulations. Recognizing that only about 15 words per grid point may be required for large eddy simulations, and that the memory projection of Toombs is about double that of the dashed line, it appears that in the early 1990's turbulent eddy simulations would be feasible—insofar as memory is concerned—with the order of 10^8 to 10^9 grid points, and by the close of the century 10^9 to 10^{10} grid points.

In contrast to the apparently bright future for memory, the technological possibilities for future growth in computer speed are dimmed by the absence of a major economic motivation for developing faster logic circuitry. The speed and complexity of current logic technology adequately meet most of the requirements of the mass market for digital watches, consumer calculators, etc. Thus there is only a relatively small economic incentive to develop improved logic chips for faster, more efficient main-frame computers. Nevertheless, the technology for random-logic integrated circuits of bi-polar ECL has improved substantially. During the past 15 years, the number of gates/chip has increased at a rate of roughly 4× per 5 years, and propagation delay decreased about 2.5× per 5 years (Fig. 23, data mainly from Anzai et al.[143]). This compounds to a rate of 10× per 5 years

for on-chip logic capability; but the improvement rate for computer speed is less due to chip-to-chip propagation delays. Costs of assembled logic have decreased 15× in 10 years (Ref. 135) equivalent to 10× per 8.5 years, essentially the same rate as the average computer-efficiency improvement trend. Turn[144] recently projected that the past trend for propagation delay will substantially continue for another decade. Chip densities for high-speed logic are currently limited by the rate that heat can be dissipated from circuit boards.

It is fortunate that at least two new technologies now in the laboratory stage—gallium arsenide and Josephson junctions—have the potential of increasing raw logic speed by over an order of magnitude. Only limited published information is available on these technologies (Refs. 145 and 146). Laboratory units of GaAs logic under development have about 10^3 gates/chip with 100 ps propagation delay, which would provide about 10 times the on-chip logic performance of the best current silicon-chips (500 gates/chip, 0.5 ns propagation delay). Heat dissipation is still an important limitation with GaAs. Superconducting Josephson junctions (JJ), with several orders of magnitude less power dissipation, essentially remove this limitation and presently are reported to have about twice the raw logic speed of GaAs digital circuits.[146] With the refinements anticipated in electron-beam lithography during the coming decade, cryogenic logic chips could conceivably have about three to four orders of magnitude greater on-chip performance. In any event, new technology now in the laboratory offers the technical potential of large improvements in digital logic speed for several decades to come. This great technical potential, unfortunately, is not currently reinforced by a driving economic incentive for development.

Figure 24 summarizes the past and projected trends in speed and cost of large computers. Computer speed developed rapidly during the early years of vacuum logic, less rapidly during the 1960's, and even less rapidly during the 1970's. A rule of thumb during the past has been "10× the speed in 5 years at twice the cost," equivalent to a cost-effectiveness improvement of 10× in 7 to 8 years (Fig. 24). This trend, shown in Fig. 24 for reference only, no longer holds for large commerical computers. A more plausible future projection for such computers would be that of roughly constant cost with speed increasing at the average computer efficiency rate of about 10× per 7 years. Such a trend, shown in Fig. 24, passes through points for the CDC 7600, Cray-1, and BSP. It is noted that the old rule of thumb (10×/5 years) happens to pass near the NASF point representing the computer speed technically feasible in the mid 1980's, and would also pass not far from a point corresponding to the potential technical capability of cryogenic systems in the 1990's. Very approximately then, the 10×/5 years curve represents roughly

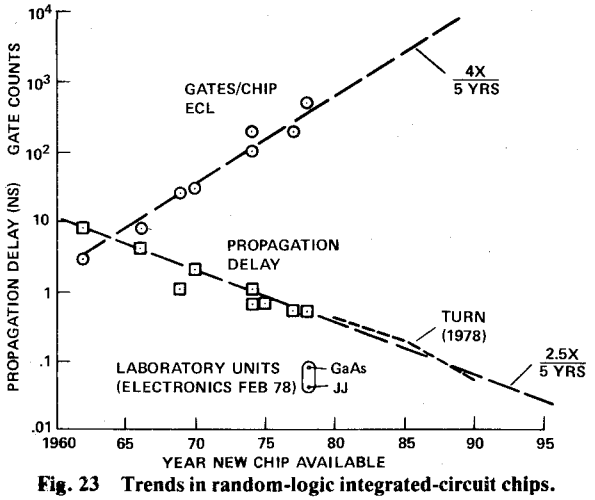

Fig. 23 Trends in random-logic integrated-circuit chips.

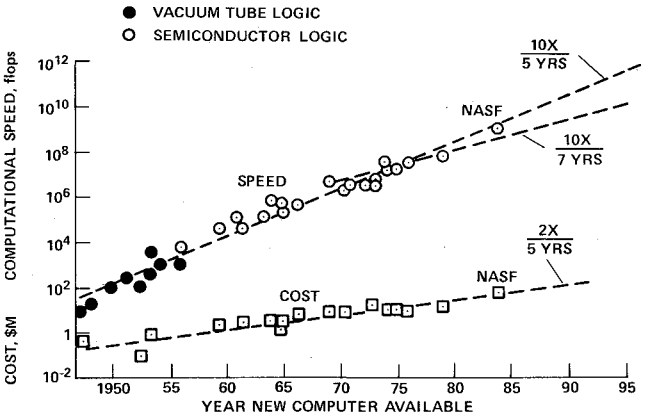

Fig. 24 Trends in speed of computation and in cost of large computers.

what appears technically feasible, whereas the 10×/7 years represents current trends for large commerical computers. Hopefully there will be sufficient stimulus in the future for the GaAs, JJ, or other new technologies such as low-temperature operation of conventional semiconductors, to provide scientific supercomputers with speed performance closer to that which is technically feasible.

It is to be noted that the general improvement in computer efficiency can be utilized in three separate ways: 1) both cost and computer power can grow, as for NASF; 2) cost can stay roughly constant while computer power grows more slowly, as for the Cray-1, BSP, and other large commerical scientific computers; 3) cost can decrease while computer power stays roughly constant, as for current desk-size modular array processor systems with roughly CDC 7600 capability.[147,148] All three serve complementary requirements: 1) for pioneering future advanced stages of very large-scale computational aerodynamics and other large-scale computations; 2) for serving the day-to-day large-scale computational needs of major institutions; and 3) for providing greatly improved, relatively low-cost computational capability for numerous individual users.

Potential Improvements in Numerical Methods

As noted earlier, past improvements in the efficiency of numerical algorithms have been large. Nevertheless, for viscous flow codes there is still much room for further improvement. The approximate number of floating point operations per grid point (Ops/GP) required to obtain a flow-field solution of the full potential transonic inviscid codes of Stage II, for example, is now the order of ten thousand. The best viscous flow codes, however, currently require the order of 10^6 Ops/GP. Interestingly, for seven different codes assessed, including both Reynolds averaged and turbulent-eddy simulation codes, the overall variation in Ops/GP was surprisingly limited, ranging from 6×10^5 to 3×10^6. Such numbers are large enough, however, to probably allow future improvements of another order of magnitude or two in the efficiency of numerical methods.

A very important aspect of numerical algorithm development is that of efficient matching to computer architecture. This represents a major challenge since the potential gains through such matching are large for vector computers. Lomax[149] has outlined how one general method (e.g., approximate factorization) can lead to algorithms for three-dimensional flows that are efficiently adapted to vector processing. When such gains are combined with inherent improvements in numerical methods, one to two orders of magnitude of overall improvement, such as has been attained during the past 10 to 15 years, does not appear unrealistic for the coming decade or two.

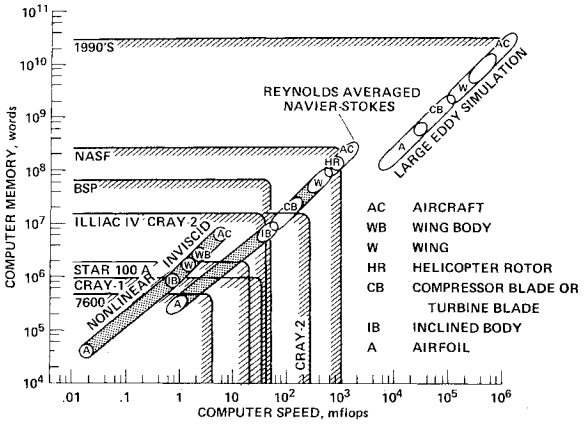

Fig. 25 Computer speed and memory requirements compared with large computer capabilities. Speed requirement based on 1-h run with 1978 algorithms.

Projected Time Scale for Advanced Simulations

By comparing the projections of future computer capability with the requirements for future advanced simulations, some interesting results are obtained, as illustrated in Fig. 25. Here the computer speed requirement in millions of floating point operations per second (MFLOPS) corresponds to simulation of a steady flow with a 1-h run using 1978 numerical methods. The range in requirements shown for a representative airfoil, wing ($\mathcal{R}=4$), and aircraft corresponds to a Reynolds number range between 10^6 and 10^8; whereas the range in requirement shown for compressor and turbine blades corresponds to the operational Reynolds number and aspect-ratio variations of different stages in a representative large jet engine. The requirements for nonlinear inviscid simulation represent transonic codes using the full potential equation, while the requirements for large eddy simulations represent computations in which subgrid scale turbulence and viscous sublayer turbulence are modeled.

The computer power estimated to be technically feasible in the mid-1980's is illustrated by the domain shown for NASF in Fig. 25. Such capability would enable numerical flowfield computations to be made on a variety of configurations of practical interest, including relatively complete aircraft (wing, body, tail, nacelles) in cruise condition at Re up to 10^8. Since a compressor- or turbine-blade flowfield requires less than 10^6 grid points, the mutual flow interactions between about 10 rotor and stator blades could be simulated without buffering between disk and semiconductor memories. It also would be practical with a capability of this magnitude to conduct numerical optimizations of individual three-dimensional turbomachinery blade shapes. Such optimization could yield significant improvements in the economics and performance of jet engines. Computer optimization of the aerodynamic shape of certain airplane components could also be made. Three-dimensional unsteady viscous compressible flow simulations, of great importance in limiting jet-engine operational boundaries and transonic aircraft maneuverability, would become amenable to practical computation with the Reynolds averaged Navier-Stokes equations. Feasible turbulent eddy simulations would be restricted to relatively simple geometries, such as airfoils and inclined bodies, and to the lower Reynolds number range of practical interest.

The feasible level of capability in the 1990's can be roughly estimated assuming that projected trends continue through this period. Such continuation may not be unrealistic. In Shepherd's judgment,[135] for example, we currently appear near the mid-point of a 12-order-of-magnitude change in computing capability with still another 5 or 6 orders of magnitude change ahead. A similar view has been expressed by Turn[144] that the incredible advances in computer capability of the past several decades will be duplicated, if not exceeded, in the coming decades. If so, turbulent eddy simulations of aerodynamic flows with the order of 10^9 to 10^{10} grid points would become feasible in the late 1990's. This represents a memory requirement of 10^2 to 10^3 times that of NASF. Since turbulent eddy simulations have grid spacings an order of magnitude smaller than Reynolds averaged simulations, they would require correspondingly smaller time steps and larger computing time; but advances in numerical methods could largely compensate for this. Hence the corresponding factor for improved computer speed beyond that of NASF would also be the order of 10^2 to 10^3. If advanced microelectronic logic technologies now in laboratories come to fruition in the coming decade, computer speeds greater than the aerodynamic requirement would become technically feasible.

The above outlook for future turbulent eddy simulation from essentially first principles is much less gloomy than previous assessments. Several factors in the present analysis contribute to this: 1) the assumption that the unresolved subgrid scale turbulence, while being slightly nonisotropic with small shear, is universal and can be modeled; 2) the presumption that the extremely small scale dynamics of the viscous sublayer very near a wall are universal and can be computed once and for all, or modeled for the practical range of physical parameters; 3) the requirement of resolving adequately turbulent energy and shear transport rather than resolving the very small dissipative eddies; and 4) the assumption of continued major improvement in computer capability and algorithm efficiency.

Analogy Between Large Eddy Simulation and Laminar Gasdynamic Computation

Numerical computations for laminar viscous flow of a gas, which generally are regarded as representing computations from first principles, embody assumptions quite analogous to those made in turbulent large eddy simulations. In both cases subgrid-scale microdynamics are modeled while large-scale dynamics are directly computed. The subgrid-scale dynamics modeled are: molecular motions in the case of laminar gasdynamics (through coefficients of viscosity and heat conduction), and dissipative eddies in the case of large eddy simulation. In both cases it is assumed that the modeled microdynamics are nonisotropic, transport small shear, are universal, have scales small relative to grid spacing, and are the mechanism of energy dissipation. Moreover, the near-wall dynamics modeled are: gas/surface molecular interactions in the case of laminar gasdynamics computation, and viscous sublayer dynamics in the case of large eddy simulation. Similarly, in both cases it is assumed that the near-wall dynamics depend only on local wall conditions, are universal, have scales small relative to boundary layer thickness, and the modeling provides the necessary velocity and temperature jumps to apply as boundary conditions to the outer flow. Thus turbulent eddy simulations as outlined above are also viewed as representing computations from essentially first principles.

Concluding Remarks

Computational aerodynamics has developed through progressive stages of increasingly refined aproximation to the full Navier-Stokes equations. The simplest stage of a linearized inviscid approximation has led to the panel methods used throughout industry for computation of subsonic flow about complex aircraft configurations. This stage now represents a relatively mature engineering tool. During the past two or three years a second stage, the nonlinear inviscid approximation, has emerged as a new engineering tool for simulating practical transonic and hypersonic flows. Within some years this second stage should

approach a maturity of treating complex configurations comparable to that now enjoyed by the panel methods. A third stage of approximation employs the Reynolds averaged Navier-Stokes equations and currently is under vigorous research development. It has opened new possibilities of treating unsteady viscous compressible flows heretofore inaccessible to detailed computation. A fourth stage of approximation involving turbulent eddy simulations from the full time-dependent Navier-Stokes equations, is currently in an early pioneering phase of research.

During the past decade, a revolutionary change has taken place in the computer market environment. The major economic incentive for developing advanced scientific super computers has essentially disappeared. Large computers now comprise only a very small fraction of the overall mass market, and no longer drive new component technologies. Nevertheless, future prospects for extensive improvements in microelectronic memory components are bright, since there is a strong mass market demand for improved memory. Although new logic technologies with great future potential are currently under laboratory development, their prospects of reaching the market as new high-speed logic components do not appear as bright, since current technology already meets most mass market requirements. Without a forceful driver, advanced high-speed logic technologies may only very slowly be brought into the market; and the entire user community interested in future advanced scientific supercomputers will be adversely affected.

Looking into the near future, it is technically feasible to assemble by the mid-1980's a computer facility (e.g., NASF) with several hundred million words of semi-conductor memory capable of simulating with the Reynolds averaged Navier-Stokes equations aerodynamic flows with 10^7 grid points in less than 2 h of computation time, or 10^6 grid points in about 10 min (using 1978 algorithms). Such a capability would make practical, for example, three-dimensional Reynolds averaged simulations of the flow over turbomachinery components, helicopter rotor blades, and aircraft configurations. It would enable two new technological capabilities to be exploited: that of using powerful computer optimization techniques to develop improved aerodynamic shapes, and that of simulating unsteady viscous flows which are of dominant importance to transonic maneuverability, turbomachinery operational limits, and stall phenomena in general. In addition, it would make practical numerical simulations using the nonlinear inviscid equations with much greater resolution and refinement of geometric detail than currently feasible.

The engineering computations feasible in the mid-1980's would be complemented by significant research capabilities for conducting "numerical experiments" with the full time-dependent Navier-Stokes equations. Although restricted to relatively simple geometries, and to the lower Reynolds numbers of aerodynamic interest, this capability would enable fundamental investigations to be made of the mechanisms of turbulence, of aerodynamic noise generation, and particularly of transition. With completely flexible control over the spectra, amplitude, and types of external disturbance imposed on a laminar flow, careful numerical experiments should shed much light on some of the transition phenomena that have long eluded comprehension and prediction.

The longer range outlook beyond the 1980's is anticipated to involve continued improvements in numerical methods and in computer power, especially memory. If projected memory trends prevail into the late 1990's, and if advanced logic technologies are stimulated to provide the corresponding requisite computer speed, turbulent eddy simulations with the order of 10^9 to 10^{10} grid points could be conducted from essentially first principles of the flow over practical aircraft configurations. Such numerical computations would entail fewer fundamental limitations than wind-tunnel experiments and should produce more accurate simulations of free-flight aerodynamics.

A key concept in the methods developed for large eddy simulation of turbulent flow is that of separating the essentially random motions of small subgrid-scale turbulence from the nonrandom motions of larger scale. Interestingly, the necessity of separating random and nonrandom processes of turbulence was emphasized 30 years ago by Dryden (Ref. 150, p. 38), who also clearly observed from the hot-wire data then available that "considerable masses of fluid move as more or less coherent units." Both of these concepts now appear fundamental to the direct numerical computation of turbulent flows.

The large turbulent eddy simulations envisioned as practical in the future would be analogous to laminar gasdynamic computations in two important ways. First, in both cases the small subgrid-scale motions are modeled as universal dynamics transporting small shear (nonisotropic but nearly-random dissipative eddies transporting small shear in large eddy simulations; nonuniform but nearly-equilibrated dissipative molecular motions transporting small shear in laminar-flow computations). Second, in both cases the very small-scale motions within an extremely thin layer adjacent to a wall are modeled as universal dynamics that depend only on local wall conditions in order to provide boundary conditions for the outer flow (velocity- and temperature-jump conditions across the thin viscous sublayer in large eddy simulations; velocity- and temperature-jump conditions across the thin gas-surface molecular interaction layer in laminar gasdynamic computations).

There are two particular areas of research in computational aerodynamics that could be explored profitably in the near future. One concerns the numerical treatment of physical phenomena contributing to the formation of unsteady flows with broadband frequency spectra. A second concerns the development of a three-dimensional time-dependent law of the wall for modeling the very small-scale dynamics of the viscous sublayer. The first would lead to immediate practical applications; the second would reduce significantly the computer power required for accurate turbulent eddy simulations.

Acknowledgments

The various examples presented of Reynolds averaged and turbulent-eddy simulations using the Navier-Stokes equations were conducted on the ILLIAC IV. I am indebted to H. Lomax, H. Bailey, G. Deiwert, T. Pulliam, J. Steger, and A. Wray for providing these examples.

References

[1] Smelt, R., "The Role of Wind Tunnels in Future Aircraft Development," *Eleventh ICAS Congress,* Lisbon, Portugal, Sept. 10-16, 1978.

[2] Chapman, D. R., Mark, H., and Pirtle, M. W., "Computers vs Wind Tunnels," *Astronautics and Aeronautics*, Vol. 13, April 1975, pp. 22-35.

[3] Ericsson, L. E. and Reding, J. P., "Reynolds Number Criticality in Dynamic Tests," AIAA Paper 78-166, Jan. 1978.

[4] Woodward, F. A., "Analysis and Design of Wing-Body Combinations at Subsonic and Supersonic Speeds," *Journal of Aircraft*, Vol. 5, June 1968, pp. 528-534.

[5] Rubbert, P. E. and Sarris, G. R., "Review and Evaluation of a Three-Dimensional Lifting Potential Flow Analysis Method for Arbitrary Configurations," AIAA Paper 72-188, 1972.

[6] Hess, J. L., "Calculation of Potential Flow about Arbitrary Three-Dimensional Lifting Bodies," Douglas Aircraft Co., Long Beach, Calif., AD 755480, Oct. 1972.

[7] Kraus, W., "Panel Methods in Aerodynamics Numerical Methods in Fluid Dynamics," Hemisphere Publication Co., 1978, pp. 237-297.

[8] da Costa, A. L., "Application of Computational Aerodynamic Methods to the Design and Analysis of Transport Aircraft," ICAS Paper, *Eleventh Congress of the International Council of the Aeronautical Sciences*, Lisbon, Portugal, Sept. 10-16, 1978.

[9] Emmons, H., "Flow of a Compressible Fluid Past a Symmetrical Airfoil in a Wind Tunnel and in Free Air," NACA TN 1746, 1948.

[10] Vincenti, W. G. and Wagoner, C. B., "Theoretical Study of the Transonic Lift of a Double-Wedge Profile with Detached Bow

Wave," NACA Report 1180, 1954.

[11] Magnus, R. and Yoshihara, H., "Inviscid Transonic Flow over Airfoils," *AIAA Journal*, Vol. 8, Dec. 1970, pp. 2157-2162.

[12] Murman, E. M. and Cole, J. D., "Calculation of Plane Steady Transonic Flows," *AIAA Journal*, Vol. 9, Jan. 1971, pp. 114-121.

[13] Steger, J. L. and Lomax, H., "Generalized Relaxation Methods Applied to Problems in Transonic Flow," *Proceedings of 2nd International Conference on Numerical Methods in Fluid Dynamics, Lecture Note in Physics*, Vol. 8, Springer-Verlag, New York, 1971.

[14] Garabedian, P. R. and Korn, D. G., "Analysis of Transonic Airfoils," *Communications on Pure and Applied Mathematics*, Vol. 24, 1971, pp. 841-851.

[15] Jameson, A., "Transonic Flow Calculations for Airfoils and Bodies of Revolution," Grumman Aerodynamics Report 370-71-1, 1971.

[16] Bailey, F. R., "Numerical Calculation of Transonic Flow about Slender Bodies of Revolution," NASA TN D-6582, 1971.

[17] Bailey, F. R. and Ballhaus, W. F., "Relaxation Methods for Transonic Flow about Wing-Cylinder Combinations and Lifting Swept Wings," *Lecture Notes in Physics*, Vol. 19, Springer-Verlag, New York, 1972, pp. 2-9.

[18] Bailey, F. R. and Ballhaus, W. F., "Comparisons of Computed and Experimental Pressures for Transonic Flows about Isolated Wings and Wing-Fuselage Combinations," NASA SP-347, Part II, March 1975, pp. 1213-1231.

[19] Reklis, R. P. and Sturek, W. B., "Computation of Transonic Flow Past Projectiles at Angle of Attack," AIAA Paper 78-1182, July 1978.

[20] South, J. C. and Jameson, A., "Relaxation Solutions for Inviscid Axisymmetric Transonic Flow over Blunt or Pointed Bodies," *Proceedings of the AIAA Computational Fluid Dynamics Conference*, Palm Springs, Calif., July 1973, pp. 8-17.

[21] Jameson, A., "Iterative Solutions of Transonic Flows over Airfoils and Wings, Including Flows at Mach 1," *Communications on Pure and Applied Mathematics*, Vol. 27, May 1974, pp. 283-309.

[22] Reyhner, T. A., "Transonic Potential Flow around Axisymmetric Inlets and Bodies at Angle of Attack," *AIAA Journal*, Vol. 15, Sept. 1977, pp. 1299-1306.

[23] Jameson, A. and Caughey, D. A., "A Finite Volume Method for Transonic Potential Flow Calculations," AIAA Paper 77-635, June 1977.

[24] Caughey, D. A. and Jameson, A., "Numerical Calculation of Transonic Potential Flow about Wing Fuselage Combinations," AIAA Paper 77-677, June 1977.

[25] Ballhaus, W. F., Jameson, A., and Albert, J., "Implicit Approximate Factorization Schemes for the Efficient Solution of Steady Transonic Flow Problems," AIAA Paper 77-634, June 1977.

[26] Holst, T. L., "An Implicit Algorithm for the Conservative Transonic Full Potential Equation Using an Arbitrary Mesh," AIAA Paper 78-113, July 1978.

[27] Gingrich, P. B., Child, R. D., and Panageas, G. N., "Aerodynamic Configuration Development of the Highly Maneuvering Aircraft Technology Remotely Piloted Research Vehicle," NASA CR 143841, June 1977.

[28] Kirk, P. S., "Summary of Wing Design Modifications for the Sabre 60 Executive Airplane," ASTEC Engineering Co., Rept. AEC-TRG-5, May 1977.

[29] Boppe, C. W., "Computational Transonic Flow about Realistic Aircraft Configuration," AIAA Paper 78-104, Jan. 1978.

[30] Hicks, R. and Henne, P. A., "Wing Design by Numerical Optimization," AIAA Paper 77-1247, Aug. 1977.

[31] Waggoner, E. G., Haney, H. P., and Ballhaus, W. E., "Computational Wing Optimization and Comparison with Experiment for a Semi-Span Wing Model," NASA TM 78480, 1978.

[32] Kutler, P. and Lomax, H., "Shock-Capturing Finite-Difference Approach to Supersonic Flows," *Journal of Spacecraft and Rockets*, Vol. 8, Dec. 1971, pp. 1175-1182.

[33] Kutler, P. and Sakell, L., "Three-Dimensional, Shock-on-Shock Interaction Problem," *AIAA Journal*, Vol. 13, Oct. 1975, pp. 1360-1367.

[34] Reinhardt, W. A., "Parallel Computation of Unsteady, Three-Dimensional, Chemically Reacting, Nonequilibrium Flow Using a Time-Split Finite-Volume Method on Illiac IV," *The Journal of Chemical Physics*, Vol. 81, No. 25, 1977, pp. 2427-2435.

[35] Peyret, R. and Viviand, H., "Computation of Viscous Compressible Flows Based on the Navier-Stokes Equations," AGARDograph No. 212, 1975.

[36] MacCormack, R. W., "Numerical Solutions of the Interaction of a Shock Wave with a Laminar Boundary Layer," *Lecture Notes In Physics*, Vol. 8, Springer-Verlag, New York, 1971, pp. 151-163.

[37] Carter, J. E., "Numerical Solutions of the Navier-Stokes Equations for Supersonic Laminar Flow over a Two-Dimensional Compression Corner," NASA TR R-385, July 1972.

[38] Jain, A. C. and Adimurthy, V., "Hypersonic Merged Stagnation Shock Layers, Part I: Adiabatic Wall Case," *AIAA Journal*, Vol. 12, March 1974, pp. 342-347.

[39] Thompson, J. F. et al., "Numerical Solution of the Unsteady Navier-Stokes Equations for Arbitrary Bodies Using Boundary-filled Curvilinear Coordiantes," *Symposium on Unsteady Aerodynamics*, R. B. Kinney, ed., University of Arizona, Tucson, 1975, pp. 453-485.

[40] Hodge, J. K. and Stone, A. L., "Numerical Solution for Airfoils Near Stall in Optimized Boundary-Fitted Curvilinear Coordinates," AIAA Paper 78-284, Jan. 1978.

[41] Tannehill, J. C., Holst, T. L., and Rakich, J. V., "Numerical Computation of Two-Dimensional Viscous Blunt Body Flows with an Impinging Shock," *AIAA Journal*, Vol. 14, Feb. 1976, pp. 204-211.

[42] Li, C. P., "A Numerical Study of Laminar Flow Separation on Blunt Flared Cones at Angle of Attack," AIAA Paper 74-585, June 1974.

[43] Shang, J. S. and Hankey, W. L., "Numerical Solution of the Navier-Stokes Equations for a Three-Dimensional Corner," *AIAA Journal*, Vol. 15, Nov. 1977, pp. 1575-1582.

[44] Hung, C. M. and MacCormack, R. W., "Numerical Solution of Supersonic Laminar Flow over a Three-Dimensional Compression Corner," AIAA Paper 77-694, June 1977.

[45] Mehta, U., "Dynamic Stall of an Oscillating Airfoil," AGARD Fluid Dynamics Panel Symposium, Ottawa, Paper No. 23, Sept. 1977.

[46] Wilcox, D. C., "Calculation of Turbulent Boundary-Layer Shock-Wave Interaction," *AIAA Journal*, Vol. 11, Nov. 1973, pp. 1592-1594.

[47] Baldwin, B. S. and MacCormack, R. W., "Numerical Solution of the Interaction of a Strong Shock Wave with a Hypersonic Turbulent Boundary Layer," AIAA Paper 74-558, June 1974.

[48] Deiwert, G. S., "Numerical Simulation of High Reynolds Number Transonic Flow," AIAA Paper 74-603, June 1974.

[49] Wilcox, D. C., "Numerical Study of Separated Turbulent Flows," AIAA Paper 74-584, June 1974.

[50] Shang, J. S. and Hankey, W. L., "Numerical Simulation for Supersonic and Hypersonic Turbulent Flow over a Compression Ramp," *AIAA Journal*, Vol. 13, Oct. 1975, pp. 1368-1374.

[51] Hung, C. M. and MacCormack, R. W., "Numerical Simulation of Supersonic and Hypersonic Turbulent Compression Corner Flows," *AIAA Journal*, Vol. 15, March 1977, pp. 410-416.

[52] Holst, T. L., "Numerical Solution of Axisymmetric Boattail Flow Fields with Plume Simulators," AIAA Paper 77-224, Jan. 1977.

[53] Levy, L. L., Jr., "An Experimental and Computational Investigation of the Steady and Unsteady Transonic Flow Field about an Airfoil in a Solid-Wall Test Channel," AIAA Paper 77-678, June 1977.

[54] Peterson, V., "Computational Aerodynamics and the Numerical Aerodynamic Simulation Facility," NASA CP 2032, 1978, pp. 5-30.

[55] Deiwert, G. S. and Bailey, H. E., "Prospects for Computing Airfoil Aerodynamics with Reynolds Averaged Navier-Stokes Codes," NASA CP 2045, 1978.

[56] Kacprzynski, J. J. and Ohman, L. H., "Wind Tunnel Tests of a Shockless Lifting Airfoil No. 1," National Research Council of Canada, NAE Project Rept. 5 × 5/0054, 1972.

[57] Kacprzynski, J. J., Ohman, L. H., Garabedian, P. R., and Korn, D. G., "Analysis of the Flow Past a Shockless Lifting Airfoil in Design and Off-Design Conditions," National Research Council of Canada, NAE Aero Rept. LR-554, Nov. 1971.

[58] Ohman, L. H., Kacprzynski, J. J., and Brown, D., "Some Results from Tests in the NAE High Reynolds Number Two-Dimensional Test Facility on Shockless and Other Airfoils," *Canadian Aeronautics and Space Journal*, Vol. 19, 1973, pp. 297-312.

[59] Steger, J. L. and Bailey, H. E., "Calculation of Transonic Aileron Buzz," AIAA Paper 79-0134, Jan. 1979.

[60] Erickson, A. L. and Stephenson, J. D., "A Suggested Method of Analyzing for Transonic Flutter of Control Surfaces Based on Available Experimental Evidence," NACA RM A7F30, Dec. 1947.

[61] Badri Narayanan, M. A. and Marvin, J. G., "On the Period of the Coherent Structure in Boundary Layers at Large Reynolds Numbers," NASA TM 78477, April 1978.

[62] Zakkay, V., Barra, V., and Wang, C., "The Nature of Boundary Layer Turbulence at High Speed," AIAA Paper 78-198, Jan. 1978.

[63] Finke, K., "Unsteady Shock-Wave Boundary-Layer Interaction on Profiles in Transonic Flow," AGARD CP 168, 1975, pp. 28-1 to 28-11.

[64] Roos, F. W. and Riddle, D. W., "Measurements of Surface Pressure and Wake-Flow Fluctuations in the Flowfield of a Whitcomb

Supercritical Airfoil," NASA TN D-8443, 1977.
[65] Coe, C. F., Riddle, D. W., and Hwang, C., "Separated-Flow Unsteady Pressures and Forces on Elastically Responding Structures," AGARD CP No. 226, 1968, pp. 2-1 to 2-25.
[66] Mabey, D. G., "Prediction of the Severity of Buffeting," AGARD LS 94, 1978, pp. 7-1 to 7-30.
[67] Dyment, A. and Gryson, P., "Etude D'Ecoulements Turbulents Subsoniques et Supercritiques par Visualisation Ultra-Rapide," AGARD CP 227, 1978, pp. 28-1 to 28-29.
[68] Sajben, M., Kroutil, J. C., and Chen, C. P., "Unsteady Transonic Flow in a Two-Dimensional Diffuser," AGARD CP 227, 1977, pp. 13-1 to 13-14.
[69] Smith, C. R., Jr. and Kline, S. J., "An Experimental Investigation of the Transitory Stall Regime in Two-Dimensional Diffusers," *Journal of Fluids Engineering, Transactions of the ASME*, Series I, Vol. 96, No. 1, March 1974, pp. 11-15.
[70] McCroskey, W. J., Carr, L. W., and McAlister, K. W., "Dynamic Stall Experiments on Oscillating Airfoils," *AIAA Journal*, Vol. 14, Jan. 1976, pp. 57-63.
[71] Hwang, C. and Pi, W. S., "Investigation of Steady and Fluctuating Pressures Associated with the Transonic Buffeting and Wing Rock of a One-Seventh Scale Model of the F-5A Aircraft," Northrup Co., Rept. NOR-78-70, 1978.
[72] Cousteix, J., Desopper, A., and Houdeville, R., "Structure and Development of a Tubulent Boundary Layer in an Oscillatory External Flow," *Symposium on Turbulent Shear Flows,* University of Pennsylvania, Philadelphia, Pa., April 1977.
[73] Hung, C. M. and MacCormack, R. W., "Numerical Solution of Three-Dimensional Shock Wave and Turbulent Boundary Layer Interaction," AIAA Paper 78-161, Jan. 1978.
[74] Shang, J. S., Hankey, W. L., and Petty, J. S., "Three-Dimensional Supersonic Interacting Turbulent Flow Along a Corner," AIAA Paper 78-1210, July 1978.
[75] Pulliam, T. H. and Lomax, H., "Simulation of Three-Dimensional Compressible Viscous Flows on the Illiac IV Computer," AIAA Paper 79-0206, Jan. 1979.
[76] Lomax, H., "Turbulence and Numerical Wind Tunnels," *Computer Science and Scientific Computing*, Academic Press, New York, 1976, pp. 127-153.
[77] Baldwin, B. S. and Lomax, H., "Thin Layer Approximation and Algebraic Model for Separated Turbulent Flows," AIAA Paper 78-257, Jan. 1978.
[78] Rubesin, M. W., "Numerical Turbulence Modeling," AGARD LS-86, 1977, pp. 3-1 to 3-37.
[79] MacCormack, R. W., "An Efficient Numerical Method for Solving the Time-Dependent Compressible Navier-Stokes Equations at High Reynolds Number," NASA TMX 73,129, July 1976.
[80] Viegas, J. R. and Horstman, C. C., "Comparison of Multiequation Turbulence Models for Several Shock-Separated Boundary-Layer Interaction Flows," AIAA Paper 78-1165, July 1978.
[81] Coakley, T. J., Viegas, J. R., and Horstman, C. C., "Evaluation of Turbulence Models for Three Primary Types of Shock Separated Boundary Layers," AIAA Paper 77-692, June 1977.
[82] Ferziger, J. H., "Large Eddy Numerical Simulations of Turbulent Flows," *AIAA Journal*, Vol. 15, Sept. 1977, pp. 1261-1267.
[83] Phillips, N. A., "The General Circulation of the Atmosphere: A Numerical Experiment," *Quarterly Journal of the Royal Meteorological Society*, Vol. 82, No. 352, 1956, pp. 123-164.
[84] Malkus, J. S. and Witt, G., "The Evolution of a Convective Element," *The Atmosphere and the Sea in Motion*, Rockefeller Institute Press, New York, 1959, pp. 425-439.
[85] Lilly, D. K., "On the Numerical Simulation of Buoyant Convection," *Tellus*, Vol. 14, 1962, pp. 148-172.
[86] Smagorinsky, J., "General Circulation Experiments with the Primitive Equations. I. The Basic Experiment," *Monthly Weather Review*, Vol. 91, No. 3, 1963, pp. 99-164.
[87] Deardorff, J. W., "A Numerical Study of Three-Dimensional Turbulent Channel Flow at Large Reynolds Numbers," *Journal of Fluid Mechanics*, Vol. 41, 1970, pp. 453-480.
[88] Deardorff, J. W., "A Three-Dimensional Numerical Investigation of the Idealized Planetary Boundary Layer," Geophysical Fluid Dynamics, Vol. 1, 1970, pp. 377-410.
[89] Grant, H. L., Stewart, R. W., and Moillet, A., "Turbulence Spectra from a Tidal Channel," *Journal of Fluid Mechanics*, Vol. 12, Pt. 2, 1962, pp. 241-268.
[90] Gibson, M. M., "Spectra of Turbulence in a Round Jet," *Journal of Fluid Mechanics*, Vol. 15, Pt. 2, 1963, pp. 161-173.
[91] Laufer, J., "The Structure of Turbulence in Fully Developed Pipe Flow," NACA Rept. 1174, 1954.
[92] Champagne, F. H., Harris, V. G., and Corrsin, S., "Experiments on Nearly Homogeneous Turbulent Shear Flow," *Journal of Fluid Mechanics*, Vol. 41, Pt. 1, pp. 81-139.
[93] Uberoi, M. S. and Freymuth, P., "Spectra of Turbulence in Wakes Behind Circular Cylinders," *The Physics of Fluids*, Vol. 12, No. 7, 1969, pp. 1359-1363.
[94] Kistler, A. L. and Vrebalovich, T., "Grid Turbulence at Large Reynolds Numbers," *Journal of Fluid Mechanics*, Vol. 26, Pt. 1, 1966, pp. 37-47.
[95] Compte-Bellot, G. and Corrsin, S., "Simple Eulerian Time Correlation at Full- and Narrow-Band Velocity Signals in Grid-Generated 'Isotropic' Turbulence," *Journal of Fluid Mechanics*, Vol. 48, Pt. 2, 1971, pp. 273-337.
[96] Sanborn, V. A. and Marshall, R. D., "Local Isotropy in Wind Tunnel Turbulence," Colorado State University, CER 65 UAS-RDM71, 1965.
[97] Tieleman, H. W., "Viscous Region of Turbulent Boundary Layer," Colorado State University, Rept. CER 67-68HWT21, 1967.
[98] Coantic, M. and Favre, A., "Activities in, and Preliminary Results of, Air-Sea Interactions Research at I.M.S.T.," *Advances in Geophysics*, Vol. 18A, 1974, pp. 391-405.
[99] Pao, Y. H., "Structure of Turbulent Velocity and Scalar Fields at Large Wave Numbers," *The Physics of Fluids*, Vol. 8, No. 6, 1965, pp. 1063-1075.
[100] Chorin, A. J., "Numerical Study of Slightly Viscous Flow," *Journal of Fluid Mechanics*, Vol. 57, Pt. 4, pp. 785-796.
[101] Leonard, A., "Simulation of Three-Dimensional Separated Flows with Vortex Filaments," *Proceedings of the 4th International Conference on Numerical Methods in Fluid Dynamics*, 1975, pp. 245-000.
[102] Orszag, S. A. and Patterson, G. S., Jr., "Numerical Simulation of Turbulence," *Lecture Notes in Physics*, Vol. 12, Springer-Verlag, New York, 1972, pp. 127-147.
[103] Fox, D. G. and Lilly, D. K., "Numerical Simulation of Turbulent Flows," *Review of Geophysics and Space Physics*, Vol. 10, No. 1, 1972, pp. 51-72.
[104] Clark, R. A., Ferziger, J. H., and Reynolds, W. C., "Evaluation of Subgrid-Scale Turbulence Models Using a Fully Simulated Turbulent Flow," Thermosciences Division, Stanford University, Rept. TF-9, 1977.
[105] Rogallo, R. S., "An Illiac Program for the Numerical Simulation of Homogeneous Incompressible Turbulence," NASA TM 73,203, 1977.
[106] Schumann, U., "Subgrid Scale Model for Finite Difference Simulations of Turbulent Flows in Plane Channels and Annuli," *Journal of Computational Physics*, Vol. 18, 1975, pp. 376-404.
[107] Grötzbach, G. and Schumann, U., "Direct Numerical Simulation of Turbulent Velocity-, Pressure-, and Temperature-Fields in Channel Flows," *Symposium on Turbulent Shear Flows*, University Park, Pa., April 18-20, 1977.
[108] Moin, P., Reynolds, W. C., and Ferziger, J. H., "Large Eddy Simulation of Incompressible Turbulent Channel Flow," Thermosciences Divsion, Stanford University, Rept. TF-12, 1978.
[109] Mansour, M. N., Ferziger, J. H., and Reynolds, W. C., "Large-Eddy Simulation of a Turbulent Mixing Layer," Thermosciences Division, Stanford University, Rept. TF-11, 1978.
[110] Orszag, S. A. and Pao, Y. H., "Numerical Computation of Turbulent Shear Flows," *Advances in Geophysics*, Vol. 18A, 1974, pp. 225-236.
[111] Wray, A., unpublished results communicated to the author, 1978.
[112] Brown, G. L. and Roshko, A., "On Density Effects and Large Structures in Turbulent Mixing Layers," *Journal of Fluid Mechanics*, Vol. 64, Pt. 4, 1974, pp. 775-816.
[113] Chandrsuda, C., Mehta, R. D., Weir, A. D., and Bradshaw, P., "Effects of Free-Stream Turbulence on Large Structure in Turbulent Mixing Layers," *Journal of Fluid Mechanics*, Vol. 85, Pt. 4, 1978, pp. 693-704.
[114] Kordulla, W., "Investigations Related to the Inviscid-Viscous Interaction in Transonic Flows about Finite 3-D Wings," AIAA Paper 77-209, Jan. 1977.
[115] Case, K. M., Dyson, F. J., Frieman, E. A., Grosch, C. E., and Perkins, F. W., "Numerical Simulation of Turbulence," Stanford Research Institute, Rept. AD-774-161, Nov. 1973.
[116] Corrsin, S., "Turbulent Flow," *American Scientist*, Vol. 49, 1961, pp. 300-325.
[117] Emmons, H. W., "Critique of Numerical Modeling of Fluid Mechanics Phenomena," *Annual Review of Fluid Mechanics*, Vol. 2, 1970, pp. 15-36.

[118] Klebanoff, P. S., "Characteristics of Turbulence in a Boundary Layer with Zero Pressure Gradient," NACA TN 3178, 1954.
[119] Ramaprian, B. R. and Shiraprasad, B. G., "The Structure of Turbulent Boundary Layers along Mildly Curved Surfaces," *Journal of Fluid Mechanics*, Vol. 85, Pt. 2, 1978, pp. 273-303.
[120] Bradshaw, P., "The Turbulence Structure of Equilibrium Boundary Layers," NPL Aerospace Rept. 1184, A.R.C. 27675, 1966.
[121] Kovasznay, L.S.G., Kibens, V., and Blackwelder, R. F., "Large-Scale Motion in the Intermittent Region of a Turbulent Boundary Layer," *Journal of Fluid Mechanics*, Vol. 41, Pt. 2, 1970, pp. 283-325.
[122] Brown, G. L. and Thomas, A.S.W., "Large Structure in a Turbulent Boundary Layer," *The Physics of Fluids*, Vol. 20, No. 10, Pt. II, 1977, pp. S243-S252.
[123] Falco, R. E., "Coherent Motions in the Outer Region of Turbulent Boundary Layers," *The Physics of Fluids*, Vol. 20, No. 10, Pt. II, 1977, pp. S124-S132.
[124] Kline, S. J., Reynolds, W. C., Schraub, F. A., and Runstadler, P. W., "The Structure of Turbulent Boundary Layers," *Journal of Fluid Mechanics*, Vol. 30, Pt. 4, 1967, pp. 741-773.
[125] Clark, J. A. and Markland, E., "Flow Visualization in Turbulent Boundary Layers," *Proceedings of the ASCE, Journal of the Hydraulics Division*, Vol. 97, No. 10, 1971, pp. 1653-1664.
[126] Blackwelder, R., "On the Role of Phase Information in Conditional Sampling," *The Physics of Fluids*, Vol. 20, No. 10, Pt. II, 1977, pp. S232-S242.
[127] Cantwell, B., Coles, D., and Dimotakis, P., "Structure and Entrainment in the Plane of Symmetry of a Turbulent Spot," *Journal of Fluid Mechanics*, Vol. 87, Pt. 4, 1978, pp. 641-672.
[128] Landahl, M. T., "Dynamics of Boundary Layer Turbulence and the Mechanism of Drag Reduction," *The Physics of Fluids*, Vol. 20, 1977, pp. S55-S63.
[129] Best, D. R., "Technology Advances and Market Forces: Their Impact on High Speed Performance Architectures," NASA CP 2032, 1978, pp. 343-353.
[130] Titsworth, J. V., "The Future of Super Computers in the U.S.," *Proceedings VIM-28*, Albuquerque, N. Mex., April 1978, pp. 191-193.
[131] Burroughs Corp., "Final Report-Numerical Aerodynamic Simulation Facility, Oct. 1977," NASA CP 2032, 1978, pp. 39-62.
[132] Lincoln, N. R., "Preliminary Study for a Numerical Aerodynamic Simulation Facility," NASA CP 2032, 1978, pp. 63-79.
[133] Spencer, R. F., Jr., "VLSI and Minicomputers," IEEE Paper CH 1328-4/78, 1978, pp. 13-25.
[134] Noyce, R. N., "Large-Scale Integration—What Is Yet to Come?," *Science*, Vol. 195, March 1977, pp. 1102-1106.
[135] Shepherd, M., Jr., "Distributed Computing Power: A Key to Productivity," *Computer*, Nov. 1977, pp. 66-74.
[136] Toombs, D., "An Update: CCD and Bubble Memories," *IEEE Spectrum*, April 1978, pp. 22-30.
[137] Hammer, C., "A Forecast of the Future of Computation," AIAA Paper 77-272, Jan. 1977.
[138] Bhandarkar, D. P., "Dynamic MOS Memories: Serial or Random Access?," IEEE Paper CH 1328-4/78-0162, 1978, pp. 162-164.
[139] Hobbs, L. C., "Hardware Technology Trends," Infotech State of the Art Report-Future Systems, Auerbach Pub. Co., 1977.
[140] Keyes, R. W., "Physical Limits on Computer Devices," IEEE Paper CH 1328-4/78-294, 1978, pp. 294-296.
[141] Charney, J. G., Fjortoft, R., and von Neumann, J., "Numerical Integration of the Barotropic Vorticity Equation," *Tellus*, Vol. 2, Nov. 1950, pp. 237-254.
[142] Fromm, J. E. and Harlow, F. H., "Numerical Solution of the Problem of Vortex Street Development," *The Physics of Fluids*, Vol. 6, No. 7, 1963, pp. 975-982.
[143] Anzai, A., Hirai, T., Takagi, R., and Nitta, T., "Developments in Subnanosecond Logic LSIs," IEEE Paper CH 1328-4/78-0178, 1978, pp. 178-182.
[144] Turn, R., "Computers in the 1980s—and Beyond," IEEE Paper CH 1328-4/78-0297, 1978, pp. 297-300.
[145] Eden, R. C., Welch, B. M., and Zucca, R., "Small Geometry Planar GaAs Integrated Circuits for Picosecond Digital Logic," IEEE Paper CH 1328-4/78-0186, 1978, pp. 186-195.
[146] "Josephson Junctions," *Electronics*, Feb. 1978, p. 43.
[147] Widhopf, G. F. and Taylor, T. D., "New Computer Technology and the Potential Impact on Fluid Dynamics and Atmospheric Pollution Studies," AIAA Paper 78-294, Feb. 1978.
[148] Steinhoff, J., "A Modular Minicomputer Based Navier-Stokes Solver," NASA CP 2032, 1978, pp. 457-470.
[149] Lomax, H., "Three-Dimensional Computational Aerodynamics in the 1980's," NASA CP 2032, Feb. 1978, pp. 33-38.
[150] Dryden, H. L., "Recent Advances in the Mechanics of Boundary Layer Flow," *Advances in Applied Mechanics*, Academic Press, New York, 1948, pp. 1-40.